Integrated Ocean Drilling Program
Expedition 306 Preliminary Report

North Atlantic Climate 2

Ice sheet–ocean atmosphere interactions on millennial timescales during the late Neogene–Quaternary using a paleointensity-assisted chronology for the North Atlantic

Documenting and monitoring bottom water temperature variations through time: installing a CORK at Site 642, Norwegian-Greenland Sea

2 March–25 April 2005

Expedition Scientists

PUBLISHER'S NOTES

Citation:
Expedition Scientists, 2005. North Atlantic climate 2. *IODP Prel. Rept.,* 306. doi:10.2204/IODP.PR.306.2005

Distribution:
Electronic copies of this series may be obtained from the Integrated Ocean Drilling Program (IODP) Publication Services homepage on the World Wide Web at iodp.tamu.edu/publications.

This publication was prepared by the Integrated Ocean Drilling Program U.S. Implementing Organization (IODP-USIO): Joint Oceanographic Institutions, Inc., Lamont-Doherty Earth Observatory of Columbia University, and Texas A&M University, as an account of work performed under the international Integrated Ocean Drilling Program, which is managed by IODP Management International (IODP-MI), Inc. Funding for the program is provided by the following agencies:

European Consortium for Ocean Research Drilling (ECORD)

Ministry of Education, Culture, Sports, Science and Technology (MEXT) of Japan

Ministry of Science and Technology (MOST), People's Republic of China

U.S. National Science Foundation (NSF)

DISCLAIMER

June 2005

The following scientists and personnel were aboard the *JOIDES Resolution* for Expedition 306 of the Integrated Ocean Drilling Program.

Expedition Scientists

Toshiya Kanamatsu
Co-Chief Scientist
Institute for Research on Earth Evolution
Japan Agency for Marine-Earth Science and Technology
2-15 Natsushima-cho
Yokosuka, Kanagawa 236-0061
Japan
toshiyak@jamstec.go.jp
Work: (81) 468-67-3832
Fax: (81) 468-67-9315

Ruediger Stein
Co-Chief Scientist
Alfred-Wegener-Institut für Polar und Meeresforschung
Columbusstrasse 2
27568 Bremerhaven
Germany
rstein@awi-bremerhaven.de
Work: (49) 471-4831-1576
Fax: (49) 471-4831-1923

Carlos A. Alvarez Zarikian
Staff Scientist/Expedition Project Manager
Integrated Ocean Drilling Program
Texas A&M University
1000 Discovery Drive
College Station TX 77845-9547
USA
zarikian@iodp.tamu.edu
Work: (979) 845-2522
Fax: (979) 845-0876

Sean M. Higgins
Logging Staff Scientist
Lamont-Doherty Earth Observatory of Columbia University
Borehole Research Group
PO Box 1000, 61 Route 9W
Palisades NY 10964
USA
sean@ldeo.columbia.edu
Work: (845) 365-8695
Fax: (845) 365-3182

Essam Aboudeshish
Logging Scientist/Physical Properties Specialist
Earth Resources Engineering Department
Graduate School of Engineering
Kyushu University
6-10-1 Hakozaki
Higashi-ku, Fukuoka 812-8581
Japan
e.aboud@mine.kyushu-u.ac.jp
Work: (81) 92 642 3643
Fax: (81) 92 642 3614

Gary D. Acton
Stratigraphic Correlator
Department of Geology
University of California, Davis
One Shields Avenue
Davis CA 95616
USA
acton@geology.ucdavis.edu
Work: (530) 752-1861
Fax: (530) 752-0951

Kazumi Akimoto
Paleontologist (foraminifers)
Center for Marine Environment Studies
Kumamoto University
Kurokami 2-39-1
Kumamoto 860-8555
Japan
akimoto@sci.kumamoto-u.ac.jp
Work: (81) 96 342 3426
Fax: (81) 96 342 3411

Ian Bailey
Sedimentologist
Earth Sciences
University College London
Gower Street
London WC1E 6BT
United Kingdom
i.bailey@ucl.ac.uk
Work: (44) 20 7679 2828
Fax: (44) 20 7679 2685

Kjell R. Bjørklund
Paleontologist (radiolarians)
Natural History Museum
Department of Geology
University of Oslo
Postboks 1172
0318 Blindern, Oslo
Norway
k.r.bjorklund@nhm.uio.no
Work: (47) 22851669
Fax: (47) 22851800

Helen Evans
Sedimentologist
Department of Geological Sciences
University of Florida
241 Williamson Hall
PO Box 112120
Gainesville FL 32611-2120
USA
geohelen@ufl.edu
Work: (352) 392-2231
Fax: (352) 392-9294

Nianqiao Fang
Sedimentologist
Center of Marine Geology
China University of Geosciences
29 Xueyuan Road
Beijing 100083
People's Republic of China
fangnq@cugb.edu.cn
Work: (86) 10-823-23501
Fax: (86) 10-823-21540

Patrizia Ferretti
Sedimentologist
Department of Earth Sciences
The Godwin Laboratory
University of Cambridge
Pembroke Street–New Museums Site
Cambridge CB2 3SA
United Kingdom
patrizia00@esc.cam.ac.uk
Work: (44) 1223 334870
Fax: (44) 1223 334871

Jens Gruetzner
Stratigraphic Correlator
Universität Bremen
Postfach 33 04 40
28334 Bremen
Germany
jgruetzn@allgeo.uni-bremen.de
Work: (49) 218-65569
Fax: (49) 421-218-65505

Yohan J.B. Guyodo
Paleomagnetist
Laboratoire des Sciences du Climat et de l'Environnement (LSCE)
Campus du CNRS
12 Ave de la Terrasse
91198 Gif-sur-Yvette Cedex
France
guyodo@lsce.cnrs-gif.fr
Work: (33) 1 69 82 3562
Fax: (33) 1 69 82 3568

Kentaro Hatakeda
Paleontologist (radiolarians)
Institute of Geology and Paleontology
Tohoku University
Aramaki Aoba, Aoba-ku
Sendai 980-8578
Japan
k_hatake@dges.tohoku.ac.jp
Work: (81) 22 217 6625
Fax: (81) 22 217 6634

Robert Harris
Physical Properties Specialist
Department of Geology and Geophysics
University of Utah
135 South 1460 East, Room 719
Salt Lake City UT 84112-0111
USA
rnharris@mines.utah.edu
Work: (801) 587-9366
Fax: (801) 581-7065

Kyoko Hagino
Paleontologist (nannofossils)
Department of Earth and Planetary Sciences
Hokkaido University N10 W8
Kita-ku, Sapporo 060-0810
Japan
hagino@nature.sci.hokudai.ac.jp
Work: (81) 11-706-4653
Fax: (81) 11-746-0394

Jens Norbert Hefter
Organic Geochemist
Geosciences
Alfred-Wegener-Institut für Polar und Meeresforschung
Columbusstrasse 2
27568 Bremerhaven
Germany
jhefter@awi-bremerhaven.de
Work: (49) 471 4831 1575
Fax: (49) 471 4831 1580

Shelley A. Judge
Sedimentologist
Department of Geological Sciences
Ohio State University
275 Mendenhall Laboratory
125 South Oval Mall
Columbus OH 43210
USA
judge.4@osu.edu
Work: (614) 292-4036
Fax: (614) 292-1496

Denise K. Kulhanek
Paleontologist (nannofossils)
Department of Geological Sciences
4100 Florida State University
108 Carraway Building
Tallahassee FL 32306-4100
USA
kulhanek@gly.fsu.edu
Work: (850) 644-6265
Fax: (850) 644-4214

Futoshi Nanayama
Sedimentologist
Institute of Geology and Geoinformation
Geological Survey of Japan, AIST
Site 7, Higashi 1-1-1
Tsukuba, Ibaraki 305-8567
Japan
nanayama-f@aist.go.jp
Work: (81) 29-861-3967
Fax: (81) 29-861-3747

Simon Nielsen
Paleontologist (diatoms)
Department of Geology
University of Florida
241 Williamson Hall
Gainesville FL 32611-2120
USA
snielsen@geology.ufl.edu
Work: (352) 392 7723
Fax: (352) 392 9294

Masao Ohno
Paleomagnetist
Graduate School of Social and Cultural Studies
Kyushu University
4-2-1 Ropponmatsu
Chuo-ku, Fukuoka 810-8560
Japan
mohno@rc.kyushu-u.ac.jp
Work: (81) 92 726 4729
Fax: (81) 92 726 4729

Harunur Rashid
Inorganic Geochemist
College of Marine Science
University of South Florida, St. Petersburg
140 Seventh Avenue South
St. Petersburg FL 33701-5016
USA
hrashid@seas.marine.usf.edu
Work: (727) 553-1538
Fax: (727) 553-1189

Francisco J. Sierro Sanchez
Paleontologist (foraminifers)
Departamento de Geología
Universidad de Salamanca
Facultad de Ciencias
37008 Salamanca
Spain
sierro@usal.es
Work: (34) 923-294497
Fax: (34) 923-294514

Antje Voelker
Paleontologist (foraminifers)
Departamento de Geologia Marinha e Costeira
Instituto Nacional de Engenharia
Tecnologia e Inovacao (INETI)
Estrada da Portela, Zambujal
2720 Alfragide
Portugal
antje.voelker@ineti.pt
Work: (351) 21-4705 567
Fax: (351) 21-471 9018

Qiumin Zhai
Sedimentologist
Earth and Planetary Science
University of Tokyo
7-3-1 Hongo
Benkyo-ku, Tokyo 113-0033
Japan
zhaiqiumin@yahoo.com
Work: (81) 3 5841 4084
Fax: (81) 3 5841 0484

Transocean Officials

Pete Mowat
Master of the Drilling Vessel
Overseas Drilling Ltd.
707 Texas Avenue South, Suite 213D
College Station TX 77840-1917
USA

Tim McCown
Drilling Superintendent
Overseas Drilling Ltd.
707 Texas Avenue South, Suite 213D
College Station TX 77840-1917
USA

IODP Shipboard Personnel and Technical Representatives

Kjell Båckvall
Weather/Ice Observer

Christopher Bennight
Research Specialist: Chemistry

Lisa Brandt
Laboratory Specialist: Chemistry

Timothy Bronk
Assistant Laboratory Officer

Paula Clark
Marine Computer Specialist

William Crawford
Imaging Specialist

John Michael Davis
Marine Computer Specialist

Jason Deardorff
Laboratory Specialist: X-ray

Randy Gjesvold
Marine Instrumentation Specialist

Burnette Hamlin
Laboratory Officer

Lisa Hawkins
Marine Laboratory Specialist: Core

Jennifer Henderson
Marine Laboratory Specialist: Paleomagnetism

Dwight Hornbacher
Applications Specialist

Karen Johnston
Marine Laboratory Specialist:
Underway Geophysics

Peter Kannberg
Marine Laboratory Specialist:
Downhole Tools/Thin Sections

Steven Kittredge
Schlumberger Engineer

Mike Meiring
Marine Instrumentation Specialist

Heather Paul
Marine Laboratory Specialist: Physical Properties

Jennifer Presley
Yeoperson

Steve Prinz
Marine Curatorial Specialist

Michael Storms
Operations Superintendent

Paul Ténierè
Assistant Laboratory Officer

ABSTRACT

The overall aim of the North Atlantic paleoceanography study of Integrated Ocean Drilling Program Expedition 306 is to place late Neogene–Quaternary climate proxies in the North Atlantic into a chronology based on a combination of geomagnetic paleointensity, stable isotope, and detrital layer stratigraphies, and in so doing, generate integrated North Atlantic millennial-scale stratigraphies for the last few million years. To reach this aim, complete sedimentary sections were drilled by multiple advanced piston coring directly south of the central Atlantic "ice-rafted debris belt" and on the southern Gardar Drift. In addition to the North Atlantic paleoceanography study, a borehole observatory was successfully installed in a new 170 m deep hole close to Ocean Drilling Program Site 642, consisting of a CORK (circulation obviation retrofit kit) to seal the borehole from the overlying ocean, a thermistor string, and a data logger to document and monitor bottom water temperature variations through time.

PREFACE

Integrated Ocean Drilling Program Expedition 306 is based on two separate proposals as follows:

(A) Proposal 572-Full3: "Ice sheet–ocean atmosphere interactions on millennial timescales during the late Neogene–Quaternary using a paleointensity-assisted chronology for the North Atlantic" and

(B) Proposal 543-Full2: "Installation of a CORK (circulation obviation retrofit kit) near Hole 642E to document and monitor bottom water temperature variations through time."

Because both parts are independent of each other, the introductory chapters of the Expedition 306 Preliminary Report (Introduction, Background, Geological Setting, and Objectives) have been divided into Part A and Part B. Sites U1312, U1313, and U1314 are related to the North Atlantic paleoceanography study (Part A), whereas Site U1315 and the revisited Ocean Drilling Program Hole 642E are related to the CORK program (Part B).

Part A: Ice sheet–ocean atmosphere interactions on millennial timescales during the late Neogene–Quaternary using a paleointensity-assisted chronology for the North Atlantic

INTRODUCTION

Following Expedition 303, Expedition 306 is the second cruise of the North Atlantic paleoceanography study, which aims to generate a late Neogene–Quaternary chronostratigraphic template for North Atlantic climate proxies, allowing their correlation at a sub-Milankovitch scale and their export to other parts of the globe by using a paleointensity-assisted chronology (PAC). The nine primary drilling locations selected for the North Atlantic paleoceanography study (Fig. **F1**) are known, either from previous Ocean Drilling Program (ODP)/Deep Sea Drilling Project (DSDP) drilling or from conventional piston cores, to have the following attributes:

- They contain distinct records of millennial-scale environmental variability (in terms of ice sheet–ocean interactions, deep circulation changes, or sea-surface conditions).
- They provide the requirements for developing a millennial-scale stratigraphy (through geomagnetic paleointensity, oxygen isotopes, microfossils, and regional environmental patterns).
- They document the details of geomagnetic field behavior.

Expedition 303, carried out in October–November 2004, occupied seven precruise sites that recovered >4600 m of high-quality Upper Pliocene–Quaternary sediments (Fig. **F1**): proposed Sites ORPH3A and ORPH2A (Sites U1302 and U1303); GAR2B (Site U1304); LAB6A, LAB7A, and LAB8C (U1305, U1306, and U1307); and IRD1A (U1308) (see the Expedition 303 *Preliminary Report* [Shipboard Scientific Party, 2005] for additional details).

Results from drilling at proposed Site LAB8C (Site U1307) during Expedition 303 established the feasibility of recovering the Pliocene sedimentary section on the Eirik Drift using the advanced piston corer (APC) system. Two holes were drilled at Site U1307 (LAB8C) reaching a maximum depth of 162 meters composite depth (mcd) in the uppermost Gilbert Chronozone (~3.6 Ma). Coring was terminated because of excessive heave when a passing storm system began to affect drilling operations. Based on the results of Expedition 303 (Channell, Stein, Malone, and Expedition Scientists, in press) and the Expeditions 303 and 306 *Scientific Prospectus* (Channell, Sato, Kan-

amatsu, Stein, Malone, and the Expedition 303/306 Project Team, 2004), Sites IRD3A and IRD4A and two sites on Eirik Drift were selected to become the primary Expedition 306 sites. The newly proposed Eirik Drift sites offered the unique opportunity to extend the Upper Pliocene–Quaternary record recovered during Expedition 303 back in time to the Miocene (see the Expeditions 303 and 306 *Scientific Prospectus Addendum* [Kanamatsu, Stein, and Alvarez Zarikian, 2005]).

Continuous weather observations performed throughout Expedition 306 showed, however, that coring operations on Eirik Drift were not possible at any time because of extremely bad weather conditions in the Labrador Sea. Thus, the alternate proposed Site GAR1B was elevated to a primary site instead. In total, we lost 10 days because of severe weather conditions in the first part of the expedition. Therefore, only three of the planned four sites related to the North Atlantic paleoceanography study were drilled during Expedition 306: proposed Sites IRD4A (U1312), IRD3A (U1313), and GAR1B (U1314) (Fig. **F1**).

BACKGROUND

The North Atlantic Ocean is undoubtedly one of the most climatically sensitive regions on Earth because the ocean-atmosphere-cryosphere system is prone to mode jumps that are triggered by changes in freshwater delivery to source areas of deep-water formation. During the last glaciation, these abrupt jumps in climate state are manifest by Dansgaard/Oeschger (D/O) cycles and Heinrich events in ice and marine sediment cores, respectively. Given the paramount importance of the North Atlantic as a driver of global climate change, we proposed to drill at nine key locations to extend the study of millennial-scale climate variability over the last few million years. What is the rationale for studying millennial-scale variability in the North Atlantic over the last few million years rather than just the last glacial cycle (recoverable by conventional piston cores)? Determining the long-term evolution of millennial-scale variability in sea-surface temperature (SST), ice sheet dynamics, and thermohaline circulation can provide clues to the mechanisms responsible for abrupt climate change. For example, the average climate state evolved toward generally colder conditions with larger ice sheets during the Pliocene–Pleistocene. This shift was accompanied by a change in the spectral character of climate proxies, from dominantly 41 to 100 k.y. periods between ~920 and 640 ka (Mudelsee and Schultz, 1997; Schmieder et al., 2000). Among the numerous questions to be answered are the following:

- When did "Heinrich events" first appear in the sedimentary record of the North Atlantic?
- Are they restricted to the "100 k.y. world" when ice volume increased substantially?

SCIENTIFIC OBJECTIVES

Climate-Related Objectives

Stratigraphy is the fundamental backbone of our understanding of Earth's history, and stratigraphic resolution is the main factor that limits the timescale of processes that can be studied in the past. Sub-Milankovitch-scale climate studies face the challenge of finding a stratigraphic method suitable for correlation at this scale (see Crowley, 1999). Even under optimal conditions, chronologies based on $\delta^{18}O$ are unable to provide sufficient stratigraphic resolution. Within the North Atlantic region, recent improvements in stratigraphic resolution have resulted in a new understanding of the dynamics of millennial-scale climate variability over the last ~100 k.y. (e.g., van Kreveld et al., 2000; Sarnthein et al., 2001). These stratigraphies have utilized chronologies from the Greenland Summit ice cores (GRIP and GISP2) and the recognition of regional lithostratigraphic linkages such as Heinrich events and higher-frequency ice-rafted debris (IRD) layers, ash layers, and susceptibility cycles combined with planktonic/benthic $\delta^{18}O$, acceleration mass spectrometry (AMS) ^{14}C dates, and geomagnetic paleointensity data (e.g., Bond et al., 1992, 1993, 1999a; Elliot et al., 2001; McManus et al., 1994; Stoner et al., 1998, 2002; Voelker et al., 1998; Kissel et al., 1999; Laj et al., 2000).

The objective of the expedition was to integrate stable isotope and relative geomagnetic paleointensity data with paleoceanographic proxies and, in doing so, generate integrated North Atlantic millennial-scale stratigraphies for the last few million years.

Understanding the mechanisms and causes of abrupt climate change is one of the major challenges in global climate change research today (see Clark et al., 1999, p. vii) and constitutes a vital initiative of the Integrated Ocean Drilling Program (IODP) Initial Science Plan. Ideally, the best approach to this problem would be to collect records of climate variability from a dense geographic network of sites, but this is impractical in paleoceanographic research. In the absence of dense coverage, the most viable approach is to obtain long continuous time series from key regions and compare the response and timing of climate change among sensitive regions. Here, we in-

tend to develop PACs to establish the phase relationships among globally distributed millennial-scale records. Building global correlations on millennial timescales is an essential step to defining the underlying mechanisms of abrupt climate change.

A persistent ~1500 y cycle has been observed for the past 80 k.y. that is apparently independent of glacial or interglacial climate state (Bond et al., 1999a). The millennial-scale cyclicity in the Holocene appears to be mirrored in the last interglacial (marine isotope Stage [MIS] 5e) and is defined by the same petrologic proxies in both interglacials. The presence of this cyclicity in interglacials, and the IRD petrology that defines it, indicates that the cyclicity does not reflect ice sheet instability or changes in calving of coastal glaciers but rather changes in sources of drifting ice, driven by changes in the size and intensity of the subpolar cyclonic gyre (Bond et al., 1999a). The Holocene cycles reflect a mechanism operating on at least a hemispheric scale (Sirocko et al., 1996; Campbell et al., 1998; deMenocal et al., 2000), indicating that the MIS 5e and Holocene cyclicities have a common origin, possibly related to solar forcing (Bond et al., 2001). The implication is that the 1500 y cycle may have been a dominant feature of the Earth's ocean-atmosphere climate over a very long time.

- How far back in time does the ~1500 y cycle extend?
- Do D/O cycles simply represent an amplification of this?
- Do distinct modes of variability persist through other glacial and interglacial intervals?
- If so, is the pacing always the same or does millennial-scale variability evolve during the late Pleistocene?

Recently published evidence from earlier interglacials (MIS 11 and 13) in both the subpolar and subtropical North Atlantic suggests that interglacial cyclicity during those times may have had a significantly longer pacing, on the order of 5000 y or more. The interglacial records from MIS 11 and 13 in Oppo et al. (1998) and McManus et al. (1999), for example, show rather sporadic events that, regardless of age model, cannot occur every 1500 y. Similarly, a MIS 11 record from ODP Site 1063 off Bermuda indicates large shifts in benthic $\delta^{13}C$ on the order of 5–6 k.y. (Poli et al., 2000). In contrast, data from MIS 11 at ODP Site 980 implies the presence of 1–2 k.y. pacing (McManus et al., 1999), suggesting that the 1500 y cycle may be operating in MIS 11 and in other pre-MIS 5e interglacials. If this is true, then the interglacial climate variability may reflect a persistent, perhaps periodic, process operating continuously within the Earth's climate (rather than noise resulting from a highly nonlinear climate system).

The best evidence for the 1500 y cycle during interglacials seems to originate from IRD proxies that monitor changes in the subpolar gyre in the North Atlantic. Our proposed drilling sites are positioned to monitor such changes. In contrast to Site 980 (Rockall Plateau), the Expedition 303 and 306 sites are located well within or close to the main present-day routes of iceberg transport into the North Atlantic and therefore are well suited to capture faint interglacial signals in shifting ocean surface circulation. If we can connect the 1500 y cycle to paleointensity records, we will have a means of directly comparing both signals with climate records from well outside the North Atlantic.

Geomagnetic-Related Objectives

Understanding the changes in the ice sheet-ocean-atmosphere system that gave rise to millennial-scale climate variability requires the precise long-distance correlation of ice cores and marine sediment cores. Geomagnetic paleointensity records from marine sediment cores have been shown to contain a global signal suitable for fine-scale correlation (see Meynadier et al., 1992; Guyodo and Valet, 1996; Channell et al., 2000; Stoner et al., 2000, 2002; Laj et al., 2000), at least for the last glacial cycle.

Beyond the range of AMS ^{14}C dating, geomagnetic paleointensity data may provide viable means of sub-Milankovitch-scale long-distance correlation. Paleointensity records have been applied to stratigraphic correlation in the Labrador Sea for the last 200 k.y. (Stoner et al., 1998), throughout the North Atlantic for the last 75 k.y. (Laj et al., 2000), and for the Atlantic realm for the last 110 k.y. (Stoner et al., 2000). As variations in geomagnetic paleointensity control atmospheric production of ^{10}Be and ^{36}Cl isotopes and the flux of these isotopes is readily measurable in ice cores, paleointensity records in marine cores provide an independent link between marine sediment and ice core records (e.g., Mazaud et al., 1994). The lows in paleointensity at ~40 and ~65 ka are readily identifiable as highs in ^{10}Be and ^{36}Cl fluxes (Baumgartner et al., 1998; Raisbeck et al., 1987) in the Greenland Summit (GRIP) and Vostok ice cores, respectively. Frank et al. (1997) showed that 10^4–10^5 y variability in ^{10}Be production rate, as determined from globally distributed deep-sea cores during the last 200 k.y., can be matched to sediment paleointensity data. This observation and the similarity of globally distributed paleointensity records indicate that much of the variability in paleointensity records is globally correlative. The few high-resolution paleointensity records available beyond 200 ka also indicate that fine-scale features are correlative. For example, the paleointensity record for the MIS 9–11 interval (300–400 ka) from the Iceland Basin (Sites 983 and 984) can be correlated to the sub-Ant-

arctic South Atlantic (ODP Site 1089) at suborbital (millennial) scale (Stoner et al., 2002).

In addition to the practical use of magnetic field records for correlation of climate records, further drilling of high-sedimentation-rate drift sites will impact the "solid Earth" theme of IODP by documenting the spatial and temporal behavior of the geomagnetic field at unprecedented resolution. Such data are required to elucidate processes in the geodynamo controlling secular variation and polarity reversal of the geomagnetic field. Recently derived records of directional secular variation and paleointensity from drift sites (e.g., ODP Legs 162 and 172) have substantially advanced our knowledge of magnetic secular variation, magnetic excursions, and directional/intensity changes at polarity reversal boundaries (see Channell and Lehman, 1997; Channell et al., 1998, 2002; Lund et al., 1998, 2001a, 2001b). Numerous directional magnetic excursions were observed within the Brunhes Chron at Leg 172 drift sites (Lund et al., 1998, 2001a, 2001b) and in the Matuyama Chron at Leg 162 sites (Channel et al., 2002). These excursions (or brief subchrons) correspond to paleointensity minima and have estimated durations of a few thousand years. Leg 162 data records and records from the Pacific Ocean suggest that spectral power at orbital frequencies in paleointensity records may reflect a fundamental property of the geodynamo (Channell et al., 1998; Yamazaki, 1999) rather than climate-related contamination of paleointensity records (Guyodo et al., 2000).

There is no doubt that North Atlantic drift sites have revolutionized our understanding of the behavior of the geomagnetic field by providing Brunhes paleomagnetic records of unprecedented resolution. These records can now provide useful constraints for numerical simulations of the geodynamo (e.g., Glatzmaier and Roberts, 1995; Gubbins, 1999; Coe et al., 2000). As a result of these parallel advances, our understanding of the geomagnetic field is on the threshold of substantial progress.

The Expedition 303 and 306 drilling sites provide high-resolution paleomagnetic records extending through the Matuyama Chron (to ~3 Ma). They will allow us to assess the temporal and spatial variability of the geomagnetic field in the Brunhes Chron and compare these records with reversed polarity records from the Matuyama Chron.

- Are the characteristics of secular variation different for the two polarity states?
- Are polarity transition fields comparable for sequential polarity reversals?

- Does the geomagnetic field exhibit a complete spectrum of behavior from high-amplitude secular variation to polarity reversals, which has not hitherto been documented because high-resolution records are lacking?

The nonaxial-dipole (NAD) components in the historical field vary on a centennial scale, and this has been interpreted to indicate similar repeat times in the past (Hulot and Le Mouël, 1994; Hongre et al., 1998). If this is correct, paleointensity records from cores with sedimentation rates less than ~10 cm/k.y. are unlikely to record anything but the axial-dipole field. On the other hand, standing NAD components have been detected in the 5 m.y. time-averaged field, although the distribution of these NAD features remains controversial (Kelley and Gubbins, 1997; Johnson and Constable, 1997; Carlut and Courtillot, 1998). Refinement of time-averaged field models as the paleomagnetic database is augmented will lead to a better grasp of how the nonzonal terms in the time-averaged field may influence paleointensity records.

RELATIONSHIP TO PREVIOUS NORTH ATLANTIC DRILLING

Prior to Expeditions 303 and 306, two ODP legs to the North Atlantic recovered sequences that are continuous and have sedimentation rates high enough to study oceanic variability on sub-Milankovitch timescales. During Leg 162, five sites (980–984) were drilled on sediment drifts south of Iceland (Fig. **F2**). These sequences are yielding invaluable insight into the nature of millennial-scale climate variability in the North Atlantic (Raymo et al., 1998, 2004; McManus et al., 1999; Raymo, 1999; Flower et al., 2000; Kleiven et al., 2003). Similarly, Leg 172 in the northwest Atlantic between ~30° and 35°N recovered sequences with high deposition rates that are suitable for millennial- and perhaps centennial-scale studies (Keigwin, Rio, Acton, et al., 1998). Given the successes of Legs 162 and 172, why are additional sites needed in the North Atlantic? The Expedition 303 and 306 sites augment those of Legs 162 and 172 in two fundamental ways. First, most of our sites are located in or close to the North Atlantic "IRD belt" (Fig. **F2**), where massive iceberg discharges are recorded in coarse layers of ice-rafted debris that are depleted in planktonic foraminifers and with oxygen isotope values indicative of reduced sea-surface salinities. Site 980 (from Leg 162) does lie within the IRD belt, but it is located on its distal northeastern edge and, consequently, lacks the strong sea-surface response to millennial-scale IRD events that are so well displayed to the south and west. Second, the depth distribution of these sites (2273–3884 meters below sea level [mbsl]) is ideal for monitoring millennial-scale changes in the production of North Atlantic Deep Water (NADW). Leg 162 sites span water

depths of 1650 to 2170 mbsl and provide the intermediate depth end-member for studies of the formation of Glacial North Atlantic Intermediate Water (GNAIW). Leg 172 drift sites provide a relatively complete depth transect spanning 1291–4595 mbsl. The Expedition 303 and 306 sites will unify the record of millennial-scale variability in the North Atlantic by bridging the "gap" between Legs 162 and 172. The sites will also expand the geographic range of sites needed to distinguish between latitudinal changes in the mixing zone between southern and northern source waters and changes due to vertical migration of water mass boundaries (Flower et al., 2000).

Data and modeling studies point to changes in the modes of NADW formation as one of the principal factors driving millennial-scale climate change in the high-latitude North Atlantic and Europe (for review, see Alley et al., 1999). Expedition 303 and 306 sites (Fig. **F1**) are distributed so that they monitor the major deepwater end-members of NADW: Norwegian-Greenland Sea Water (Site U1304) and Labrador Sea Water (Sites U1305–U1307) as well as the final NADW mixture (Sites U1302 and U1303). Alley et al. (1999) discussed three distinct modes of thermohaline circulation in the North Atlantic: modern (M), glacial (G), and Heinrich (H). The modern mode is marked by deepwater formation in the Nordic Seas and North Atlantic where the three end-members mix to form NADW. In the glacial mode, deepwater formation is suppressed in the Nordic Seas and GNAIW forms farther south in the North Atlantic. In the Heinrich mode, both deep- and intermediate-water formation is greatly reduced. Together with the depth transects drilled during Legs 162 and 172, the Expedition 303 and 306 sites permit monitoring deep- and intermediate-water formation during all three circulation modes.

DRILLING STRATEGY

The (high resolution) stratigraphic goals require high sedimentation rates (>5 cm/k.y.) at the chosen sites, as well as complete and undisturbed recovery of the stratigraphic sequence. The drilling strategy remained the same as that during Expedition 303 and consisted of APC coring in three or more holes at each site to ensure complete and undisturbed recovery of the stratigraphic section. We used the "drillover" strategy employed during ODP Leg 202 to maximize APC recovery and penetration. Traditionally, the depth limit of APC coring is controlled by the overpull required to retrieve the core barrel. In cases where the full APC stroke is achieved but excessive force is required to retrieve the core barrel (often the limit of APC penetration), the drillover strategy entails advance of the rotary bit to free the APC barrel. APC coring

was generally terminated when the pressure gauge on the rig floor indicated that full APC stroke could no longer be achieved. Because of the pivotal role of magnetic studies in the objectives of the proposal, nonmagnetic core barrels were generally used. However, because of the relative fragility and high cost of nonmagnetic core barrels, the normal steel magnetic barrels were used after the initiation of drillover.

Two factors influenced the decision to terminate holes at the limit of the APC and therefore *not* to utilize extended core barrel (XCB) technique:

- The increase in drilling disturbance associated with the XCB, particularly in the upper part of the XCB section, has not been conducive to the generation of high-resolution PACs. Poor recovery and "biscuiting" are common in poorly consolidated lithologies recovered by XCB.
- At all locations, other than Site U1314, the deeper stratigraphic section was sampled in the region during DSDP Leg 94.

Part B: Installation of a CORK near Hole 642E to Document and Monitor Bottom Water Temperature Variations through Time

INTRODUCTION

The northern North Atlantic is the primary deep ventilator of the oceans, and it is now recognized that production of deep water in the northern North Atlantic is intimately related to the global climate (Broecker, 1987; Dickson, 1997; Woods et al., 1999). Changes in the production of NADW may be the result of, or lead to, regional or global climatic changes. Unfortunately there is a lack of long-term temperature observations, and those that do extend back in time are concentrated at the surface or near the surface. Hydrographic time series from the North Atlantic, though sparse and sporadic, show natural variability on timescales of decades to centuries (Wunsch, 1992). In the deep ocean, the few observations that do exist show variability on similar timescales and at large spatial scales. Oceanographic observations indicate that the thermohaline structure of the North Atlantic has changed during the past 20 to 30 y, indicating the presence of significant variations in bottom water temperature (BWT) (Roemmich and Wunsch, 1984; Antonov, 1993).

BACKGROUND

It is hypothesized that subbottom temperature-depth profiles can be used to construct BWT histories at timescales on the order of decades to a century. The conductive thermal regime of oceanic crust comprises the superposition of two processes: the outward flow of heat from the Earth's deep interior and perturbations to the deep regime by changes of BWT at the seafloor. The latter effects operate on a relatively short timescale (decades, centuries, and millennia), whereas the former process operates on a geologic timescale, with secular changes taking place over millions of years. In the context of short-term BWT perturbations, outward flow of heat from the interior is seen as a quasi-steady-state process. Because oceanic sediments have a low thermal diffusivity, changes in BWT diffuse slowly downward by conduction, perturbing the background thermal regime. These measurable anomalies are a direct thermophysical consequence of BWT variations, and as such are a straightforward measure of temperature, not a proxy. Resolution analysis indicates that 100 y of temperature change is potentially recoverable from high-precision temperature-depth logs in boreholes 200 m deep. If this hypothesis is correct, and because ocean bottom sediments continuously record changes in BWT, it is theoretically possible to reconstruct BWT histories anywhere in the ocean.

Site 642 (Fig. **F3**) represents an ideal candidate to test this hypothesis for two reasons. First, it is located near Ocean Weather Ship Station (OWS) Mike, which has been in continuous operation during the last 50 y. Weekly temperature and salinity measurements at depths >2000 m have been made since 1948 (Gammelsrød et al., 1992). These measurements represent the longest homogeneous time series from the deep ocean. They will be used to check the efficacy of our measurements and analysis as well as to provide a direct test of our hypothesis. Second, it is located on the eastern margin of the Norwegian Sea (Fig. **F3**), a climatically sensitive area that records the changing hydrographic character and horizontal exchange of deep water from the Greenland Sea, Arctic Ocean, and Norwegian Sea. As such, BWT histories will yield insight into the complex interplay between these important water masses.

SCIENTIFIC OBJECTIVES

The primary objectives of this study are

- To document the ability to recover BWT histories from temperature depth profiles. The possibility to reconstruct BWT histories with sufficient resolution creates the

potential for transects of such measurements across climatologically important gateways such as the Reykjanes Ridge.

- To reconstruct BWT histories at Site 642. How large have these variations been? How far back in time can we reliably estimate BWT histories?
- To isolate perturbations in the subsurface temperature profile resulting from variations in BWT histories. Are observed temperature perturbations to the background thermal field in fact due to variations in BWT?

PROPOSED RESEARCH

To capture thermal transients associated with temporal variations in BWT, we envisioned a borehole observatory in a new 180 m hole close to Site 642, consisting of a CORK to seal the borehole from the overlying ocean and a thermistor string and data logger to make and record temperature measurements. This configuration allows high-precision temperature measurements as a function of both depth and time. High-precision temperature measurements will be made at two timescales: in quick succession and over longer time intervals. Averaging a quick succession of temperature measurements is an effective way to reduce instrumental and environmental noise. Temperature measurements with an appropriate length of time between them can be used to directly monitor the propagation of transient temperatures (Chapman and Harris, 1992).

OPERATIONS STRATEGY

At 67°12.7′ N, 02°56.2′ E (water depth = 1289 m) near Hole 642E, operations began by drilling to ~180 meters below seafloor (mbsf) with $10^3/_4$ inch casing and reentry cone. The bottom of the cased hole was sealed with cement to ensure against formation fluids entering the borehole interval where the measurements are made, and then the CORK and thermistor string were installed.

The operational plan for the new hole at Site 642 precluded a logging program in that hole. To assess current background thermal conditions in the region, however, a downhole record of temperature from Hole 642E was obtained using the Lamont-Doherty Earth Observatory (LDEO) high-temperature tool. In addition to the temperature tool, the triple combination (triple combo) and Formation MicroScanner (FMS) tool strings were run.

PRINCIPAL RESULTS

Site U1312

Site U1312 (proposed Site IRD4A) constitutes a reoccupation of DSDP Site 608 located northeast of the Azores Islands (Portugal) on the southern flank of the King's Trough tectonic complex at a water depth of 3554 m (Fig. **F1**). Two principal holes (Holes 608 and 608A) were drilled to 515.4 and 146.4 mbsf, respectively, with the variable-length piston coring (VLHPC) system and the XCB during DSDP Leg 94 (June–August 1983) (Ruddiman, Kidd, Thomas, et al., 1987). At this site, a nearly continuous bio- and magnetostratigraphic section of Quaternary to mid–upper Oligocene sediments was recovered to 455 mbsf (Baldauf et al., 1987). Below this depth, some coring gaps and the presence of a major hiatus representing at least 7.5 m.y. (late Eocene–early Oligocene) cause the record to be less complete through the Oligocene and into the Eocene. Upper middle Eocene (Zone NP16) sediments lie upon the basaltic basement at 515.4 mbsf. Mean sedimentation rates at DSDP Site 608 are 2–3 cm/k.y., with the higher values generally occurring in the late Neogene/Quaternary time intervals. Incomplete recovery and the present condition of the existing DSDP cores collected in 1983 do not permit the detailed paleoceanographic studies proposed here. The main objective at Site U1312 was to obtain continuous records of surface and deepwater characteristics and their interactions with ice sheet instabilities during Neogene-Quaternary times. In this context, an important target at this site was the recovery of a complete undisturbed upper Miocene section by means of APC coring.

Two holes were cored with the APC system and nonmagnetic core barrels at Site U1312. Hole U1312A was drilled to a maximum depth of 237.5 mbsf, with a recovery of 104.5% (Fig. **F4**). In this hole, the "drillover" technique was required for recovery of Cores 306-U1312A-23H through 25H. Because of excessive heave (≥5 m), initial coring conditions were not optimum. This prevented the recovery of a good mudline in Hole U1312A, and the first several cores (306-U1312A-1H through 3H and 5H) were disturbed by flow-in. Hole U1312B was drilled to a maximum depth of 231.9 mbsf, with a recovery of 102.1% (Fig. **F4**). In Hole U1312B, a successful mudline was achieved during a period of reduced heave and drillover was required only for the recovery of Core 306-U1312B-25H. Drilling of a third hole was precluded as weather conditions dramatically deteriorated.

The sedimentary succession at Site U1312 consists of Holocene to upper Miocene sediments with varying mixtures of biogenic and detrital components, primarily nanno-

fossils, foraminifers, and clay minerals (Fig. F4). Two lithologic units were distinguished based on sediment color, carbonate content, reflectance values, and the occurrence of detrital components. Unit I (0–79.70 mbsf; Holocene to Late Pliocene) is dominated by nannofossil ooze, foraminifer nannofossil ooze, nannofossil ooze with silty clay, and silty clay nannofossil ooze. Alternating diffuse color bands occur throughout much of the unit. Most contacts between the various lithologies are gradational and/or bioturbated. Unit I was further subdivided into two subunits. Subunit IA exhibits high-amplitude variations in magnetic susceptibility and carbonate content, whereas in Subunit IB these variations are less distinct. Dropstones are generally rare and small (2–15 mm in diameter) and are concentrated in the upper 23 m of Subunit IA. Unit II (79.70–232.05 mbsf; Late Pliocene to late Miocene) is dominated by nannofossil ooze that exhibits little color change due to a downhole decrease in abundance of both detrital content and diffuse color bands.

Abundant, generally well preserved calcareous nannofossils and planktonic foraminifers occur throughout both holes at Site U1312. Planktonic foraminifer assemblages are mainly composed of temperate to subpolar species, with some sporadic incursions of polar and subtropical taxa. Nannofossil assemblages consist of cosmopolitan species typical of the North Atlantic at mid-latitude. A reliable chronostratigraphic framework spanning from the late Miocene (~11 Ma) to the present was established based on the succession of bio-events identified in the cores (Table T1). Linear sedimentation rates were estimated based on the depth of these events. Average sedimentation rates were low during the late Miocene (1–2 cm/k.y.), increased in the Early Pliocene (2.5–6 cm/k.y.), and decreased again in the latest Pliocene and Pleistocene (1.5–2 cm/k.y.) (Fig. F5). Although calcareous plankton species were usually well preserved, intense fragmentation of planktonic foraminifer shells and overgrown discoasters were observed in the uppermost Miocene (161–171 mbsf in Hole U1312A and 165–175 mbsf in Hole U1312B), coinciding with an interval of very low sedimentation rates. The occurrence of a hiatus due to carbonate dissolution in this part of the record is probable because several bioevents were observed in the same core. A similar interval with extremely low sedimentation rates and/or a possible hiatus but good carbonate preservation was also observed in the Upper Pliocene–lower Pleistocene (38–47 mbsf in Hole U1312A and 32–41 mbsf in Hole U1312B). Nannofossils recovered from this interval in Hole U1312B indicate an age older than planktonic foraminifers from the same horizon, further suggesting the presence of a hiatus or significant reworking.

Biostratigraphy based on siliceous fossils was hindered by rare occurrences and dissolution of radiolarians and diatoms. Trace numbers of diatoms are present in the upper ~60 m of both holes, and show an age-depth progression similar to the calcareous nannofossils. Below 60 mbsf, the sediments are almost entirely barren of diatoms. Likewise, radiolarians are found in trace numbers down to a depth of 85.5 mbsf in Hole U1312A and 114 mbsf in Hole U1312B. Only one radiolarian event was observed in Hole U1312A, and only samples at 28.5 and 37.5 mbsf contained rich radiolarian faunas in Hole U1312B.

The magnetic interpretations at Site U1312 were based on measurements of the natural remanent magnetization (NRM) after alternating-field (AF) demagnetization at a peak field of 20 mT. The Brunhes/Matuyama reversal occurs at 18.40 mbsf in Hole U1312A and at 16.95 mbsf in Hole U1312B. The Jaramillo Subchron occurs between 20.90 and 24.80 mbsf in Hole U1312B. In Hole U1312B, the Gauss/Matuyama and Gauss/Gilbert boundaries were tentatively placed at 51.60 and 72.2 mbsf, respectively, although a significant part of the Gauss interval (Chron C2An) is missing because of coring-induced sediment deformation. NRM intensities fall in the range of 10^{-5} A/m between ~100 and 210 mbsf in both holes. This range is close enough to the noise level of the magnetometer that establishing a continuous magnetostratigraphy was not possible by shipboard measurements. A long interval of normal polarity at the bottom of Holes U1312A and U1312B (top at 207.6 and 204.7 mbsf, respectively) was tentatively identified as Chron C5n (Fig. **F6**).

A complete splice of the entire sedimentary section at Site U1312 was difficult to construct because only two holes were cored and much of the upper portion of Hole U1312A was affected by coring disturbance. The remanent magnetic intensity following 20 mT AF demagnetization and the lightness (L*) parameter from color reflectance measurements proved to be the most useful for correlating between holes down to 158.89 mcd (the bottom of Core 306-U1312B-16H). Below 158.89 mcd, stratigraphic correlation was difficult because of the very uniform sediment composition, resulting in few diagnostic variations in physical properties. From 158.89 up to 68.05 mcd, between-hole correlation was good and all core breaks could be filled, resulting in a complete splice. Above this, several gaps occur between core breaks and much of the spliced section is built from Hole U1312B cores, which contained virtually no coring deformation within this interval. From 0 to 40 mcd, L* variations, which mainly reflect the carbonate content, mirror variations observed in the 0–1.5 Ma portion of benthic oxygen isotope stacks. Sedimentation rates derived from this correlation vary between 0.5 and 3.5 cm/k.y. during the past 1.5 m.y.

Alkalinity of the pore water in the upper 110 m exhibits a continuous trend in increasing values downhole to a depth of ~80 mbsf, followed by a decrease thereafter. In contrast, chlorinity decreases with depth. The highest silica value of ~650 µM was measured at 53.5 mbsf. Barium exhibits its highest values (0.7 µM) at 82 mbsf, just below the boundary between lithologic Units I and II.

Carbonate concentrations in the sedimentary record at Hole U1312A range from 59 to 98 wt% (average = 90.4 wt%). Highest values (92–98 wt%) are observed in the lower part of the record (more than ~55 mbsf), whereas the uppermost ~55 m (lithologic Subunit IA) are characterized by lower values and high variability. Two discrete intervals of decreased $CaCO_3$ values (82 wt%) occurred at 81.95 and 110.45 mbsf. A similar trend was observed in the overall $CaCO_3$ concentration at DSDP Site 608. Total organic carbon varies between 0 and 0.9 wt%, with the lowest values (0–0.1 wt%) found below 85 mbsf and higher and more variable values (0.1–0.9 wt%) found above. Total nitrogen is low and relatively constant throughout the hole (~0.1 wt%).

Physical property measurements at Site U1312 included nondestructive measurements of magnetic susceptibility, density, and natural gamma radiation (Fig. **F7**). Working sections were used to measure moisture and density (MAD) and compressional *P*-wave velocity. These properties generally show greatest variability in the upper 40 m, consistent with greater clay content, and generally show lower values with depth, except for density and *P*-wave velocity, which increase with depth.

Site U1312 accomplished near full recovery of the excellent upper Miocene section first drilled at DSDP Site 608. The sedimentary sequence representing the last ~11 m.y. will allow the study of short- and long-term climate variability and ocean-atmosphere interactions under very different boundary conditions, such as the closure and reopening of Atlantic/Mediterranean connections at the end of the Miocene (6–5 Ma), the closing of the Isthmus of Panama (4.5–3 Ma), and the onset of major northern hemisphere glaciation near 2.5 Ma.

Site U1313

IODP Site U1313 (proposed Site IRD3A) constitutes a reoccupation of DSDP Site 607 located at the base of the upper western flank of the Mid-Atlantic Ridge in a water depth of 3426 m, ~240 miles northwest of the Azores Islands. Two holes were drilled at this site during Leg 94 using the VLHPC system and the XCB system (Ruddiman, Kidd, Thomas, et al., 1987). Hole 607 penetrated to a total depth of 284.4 m, and Hole

607A penetrated to a total depth of 311.3 m. The sediments recovered at Site 607 predominantly consist of calcareous biogenic oozes with variable amounts of fine-grained terrigenous material. Based on magneto- and biostratigraphy, the mean sedimentation rate at Site 607 is ~5 cm/k.y. for the Pliocene–Pleistocene time interval.

The rationale for reoccupying this site is essentially the same as for Site U1308 (re-coring of DSDP Site 609) (see Channell, Sato, Malone, and Expedition Scientists, in press). Together Sites 607 and 609 constitute benchmark sites for long-term (millions of years), as well as short-term, surface and deep ocean climate records from the subpolar North Atlantic. These sites, today situated under the influence of the NADW, have been very important for generating benthic $\delta^{18}O$, $\delta^{13}C$, and $CaCO_3$ records for the Pleistocene (Ruddiman et al., 1989) and Late Pliocene (Ruddiman et al., 1986; Raymo et al., 1989, 2004), for interpreting these records in terms of ice sheet variability and changes in NADW circulation, and for generating orbitally tuned timescales. Site 607, at a water depth of 3427 m, remains the only site in the high-latitude North Atlantic that monitors NADW circulation throughout the Pleistocene.

Reconstruction of sea-surface temperature (SST) in the North Atlantic indicates that the polar front was situated at ~42°–46°N during glacial times, extending in an east–west direction and resulting in a steep south–north SST gradient (CLIMAP, 1976; Pflaumann et al., 2003). Alkenone SST estimates determined in sediment cores from areas south of and within the Polar Front resulted in very different values for different glacials (Calvo et al., 2001), indicating different climatic conditions (e.g., the location of the Polar Front) during these glacial periods. At the site of Core VM 30-97, located close to Site 607 (Fig. **F2**), Heinrich events are marked by distinctive detrital carbonate signature and planktonic foraminifer-derived SSTs warmed markedly during the Heinrich events and during the Last Glacial Maximum, in distinct contrast to climate records from the subpolar North Atlantic (Bond et al., 1999b).

Site U1313 (especially in combination with similar records from other Expedition 303/306 sites) will document the evolution of complex surface-temperature phasing over the last few million years. By placing the surface temperature signals into a chronological framework based on a combination of oxygen isotope stratigraphy, detrital carbonate-bearing Heinrich events, and geomagnetic paleointensity, we expect to obtain an optimal reconstruction of the phasing of temperature records and their relationship to ice sheet instability and changes in deepwater circulation on millennial to submillennial timescales.

Four holes (Holes U1313A, U1313B, U1313C, and U1313D) were cored with the APC system and nonmagnetic core barrels to maximum depths of 308.6, 302.4, 293.4, and 152.0 mbsf, respectively (Fig. **F7**). The average recovery was 103.5%. In Holes U1313A and U1313C, drillover was required for recovery of the last two and four cores, respectively. After completing coring operations in Hole U1313B, the hole was prepared for logging and the triple combo tool string was deployed (including the General Purpose Inclinometer Tool [GPIT] and Multi-Sensor Spectral Gamma Ray Tool [MGT]) to 2.0 m off the bottom of the hole. The entire 300 m sequence was successfully logged.

The Holocene to uppermost Miocene sedimentary succession at Site U1313 consists primarily of nannofossil ooze with varying amounts of foraminifers and clay- to gravel-sized terrigenous components (Fig. **F4**). Two major lithologic units were identified. Unit I (0–111.86 mbsf in Hole U1313A, 0–111.28 mbsf in Hole U1313B, 0–112.00 mbsf in Hole U1313C, and 0–113.14 mbsf in Hole U1313D) consists of Holocene to Upper Pliocene alternating nannofossil ooze, silty clay nannofossil ooze, and nannofossil ooze with clay. Regular occurrences of dropstones in Unit I demonstrate that northern hemisphere ice sheet instability played a role in the sediment's paleoclimate record during the Pleistocene to Late Pliocene. Unit I can be further subdivided into two subunits. Subunit IA exhibits the largest amplitude fluctuations in detrital clay and biogenic carbonate, reflected by distinct color changes and shifts in L* (Fig. **F8**), weight percent carbonate, gamma ray attenuation (GRA) density, and magnetic susceptibility, whereas Subunit IB is defined by decreased variability in these components. Millimeter- to centimeter-scale pale green color bands are distributed throughout the succession, and a horizon of reworked volcanic ash can be correlated across all holes in Subunit IA. Unit II extends to the bottom of each hole (111.86–308.42 mbsf in Hole U1313A, 111.28–302.52 mbsf in Hole U1313B, 112.00–293.33 mbsf in Hole U1313C, and 113.14–153.0 mbsf in Hole U1313D). Unit II is very homogeneous and differs mainly from Unit I in its smaller terrigenous component, which decreases gradually downhole from the unit boundary to ~150 mbsf. Unit II consists of Upper Pliocene to uppermost Miocene nannofossil ooze and is characterized by high and stable carbonate concentrations. Discrete patches and streaks of pyrite occur throughout this unit and are probably related to local reducing conditions associated with organic matter complexes. Pale green color bands are prevalent in the otherwise nearly white sediment.

Site U1313 yielded abundant assemblages of calcareous microfossils spanning the late Miocene to Holocene. Biohorizons based on calcareous microfossils closely match ages based on paleomagnetic data for the Pliocene and Pleistocene, and indicate

nearly constant sedimentation rates of 4–5 cm/k.y. throughout this time interval (Fig. F5). The oldest sediments at Site U1313 are tentatively dated at 6.0 Ma based on a nannofossil last occurrence near the base of Holes U1313A and U1313C, a tentative planktonic foraminifer event at the base of Hole U1313A, and a possible diatom event in Core 306-U1313C-32H (Table T1). Based on these biohorizons, sedimentation rates in the late Miocene are ~13–14 cm/k.y. (Fig. F5).

Calcareous nannofossils are well preserved throughout much of the section, although some dissolution and overgrowth is present within the upper Miocene. Pleistocene sediments contain very minor amounts of reworked nannofossils. Planktonic foraminifers are moderately to well preserved and reveal a high faunal diversity including several (sub)tropical species. An incursion of encrusted *Neogloboquadrina atlantica* (dextral) occurs in the early Pleistocene, making this the youngest occurrence of this species in the mid-latitude North Atlantic.

Radiolarians at Site U1313 reveal great variation in abundance, state of preservation, and faunal associations among the four holes. In general, radiolarians are abundant and well preserved in the upper five to six core catcher samples, whereas dissolution is severe in the lower part. *Cycladophora davisiana* is found in samples up to 14 cores deeper than its anticipated first occurrence in the North Atlantic at 2.6 Ma. If these occurrences are real and not a result of downhole contamination, then the first occurrence of *C. davisiana* is ~5.5 Ma.

A diverse warm-water diatom flora is generally present within the upper 40–70 mbsf during the Pliocene–Pleistocene intervals, containing a mixture of Arctic and Subarctic, possibly ice-rafted species. However, diatoms are only abundant in the first two core catchers and occur only as traces below 50–60 mbsf. When present, warm-water diatoms are generally well preserved, but often fragmented. The diatoms from colder water masses are usually partially dissolved.

The magnetostratigraphy at Site U1313 was constructed on the basis of continuous NRM measurements after AF demagnetization at a peak field of 20 mT. NRM intensities after 20 mT AF demagnetization are in the range of 10^{-3} to 10^{-4} A/m above 150 mbsf but fall to the range of 10^{-5} A/m in the lower part of the section. The sediments provide a good record of the Brunhes, Matuyama, and Gauss polarity intervals down to ~150 mbsf (Fig. F6). Below this depth, the inclination signal is noisier but alternating intervals of normal and reversed polarities can still be defined with confidence down to ~250 mbsf. The magnetostratigraphy is uncertain below this depth, as it var-

ies from one hole to the other, partly because the stronger drill string overprint induced by alloy steel core barrels used in the lowermost part of Holes U1313A and U1313C. The magnetostratigraphy is consistent with the biostratigraphy from the top down to ~220 mbsf. In the underlying sediment, however, the link to the biostratigraphy is not straightforward (Fig. **F5**).

The four holes cored at Site U1313 provided ample sediment for constructing one complete spliced stratigraphic section and a second nearly complete section. Correlation between holes was excellent in the upper 168.5 mcd because of pronounced variations in nearly all physical properties measured. In particular, L* from color reflectance measurements mimics variations in the global benthic oxygen isotope stack (e.g., Lisiecki and Raymo, 2005), and a preliminary age model was constructed by matching sharp L* variations with glacial and interglacial terminations. Between-hole correlation was more difficult below 168.5 mcd (~151 mbsf) because the sediments are fairly homogeneous calcareous nannofossil ooze.

Apart from general trends, most pore water chemical constituents show a notable change between ~80 and 110 mbsf (i.e., at the lithologic Unit I–II transition). Alkalinity and Sr^{2+} increase downhole, whereas the Li^{+} decreases. The highest dissolved silica content of ~563 µM is measured at 39.3 mbsf. SO_4^{2-} concentration exhibits a slight downhole decrease from ~26 to 24 µM, whereas the NH_4^{+} shows the opposite trend (126–418 µM, with a high value of 615 µM at 47.8 mbsf). Ba^{2+} shows a more or less uniform concentration (~3.2 µM) throughout the profile.

Carbonate concentrations in the sediments of Hole U1313A range from 31.5 to 96.7 wt% (average = 80.5 wt%). Relatively uniform and high values (>90 wt%) are observed below ~120 mbsf (Unit II), whereas the top ~120 mbsf (Unit I) is characterized by distinct and strong variations (30–90 wt%). Maximum amplitude with as much as 60 wt% difference in $CaCO_3$ occurs in the uppermost 40 mbsf, whereas the amplitude of variation is reduced to 40–50 wt% from 40 to 120 mbsf. Similar general features of the $CaCO_3$ variability were observed at Site 607. Total organic carbon (TOC) varies between 0 and 0.65 wt%, with the lowest values (<0.1 wt%) below 170 mbsf but higher and more variable values (0.1–0.65 wt%) above. Total nitrogen is low and relatively constant throughout the hole (0.1–0.15 wt%). Preliminary results from a limited number of samples (16) show that solvent-extractable organic matter at Site U1313 consists primarily of odd-numbered C_{25}–C_{35} *n*-alkanes and long-chain C_{37}–C_{40} alkenones. Variations in proportions of these compound classes reflect a change in the organic matter composition with respect to terrigenous and marine sources.

Alkenone-derived SSTs show variability from ~13° to 19°C during the Pleistocene, whereas temperatures of ~20° and 22°C are obtained for the Late Pliocene and the latest Miocene, respectively.

Physical properties measured at Site U1313 include magnetic susceptibility (by multisensor track [MST] and multisensor core logger [MSCL]), GRA density, *P*-wave velocity, and natural gamma radiation using the MST. In addition, the porosity and density were measured on discrete samples by MAD. Finally, *P*-wave velocities were measured in the x-direction using the *P*-wave sensor (PWS3). The results show a large variability of all physical properties in the upper ~120–140 m, which is probably related to the variation of clay content in the upper sediments (Figs. **F4, F8**). Below 120 mbsf, the variability in physical properties is small as a result of the very high carbonate content (>95 wt%).

Site U1313 (especially in combination with similar records from other Expedition 303/306 sites) will document the evolution of complex surface-temperature phasing over time, addressing questions such as whether the patterns are a peculiarity of the last glaciation, whether they were present in the 41 k.y. world, and whether they appeared at the onset of northern hemisphere glaciation. By placing the surface-temperature signals into a chronological framework based on a combination of oxygen isotopic stratigraphy, detrital carbonate-bearing IRD (Heinrich-type) events, and geomagnetic paleointensity, we expect to obtain an optimal reconstruction of the phasing of the temperature records and its relationship to ice sheet instability and changes in deepwater circulation.

Downhole Logging of Hole U1313B

The successful deployment of the triple combo tool string in Hole U1313B provided complete coverage of the 300 m section and provided very good physical property and lithologic information for density, porosity, natural gamma radiation, resistivity, and photoelectric effect. Corresponding core physical property measurements were very consistent with in situ downhole data. Of special note is the dramatically consistent linear correlation of downhole natural gamma radiation (upper 225 mbsf) with the recent Lisiecki and Raymo (2005) benthic oxygen isotope record of the last 5.4 m.y. The consistency of downhole data with both core data and age models will allow mapping of the spliced core record to actual depth, resulting in more accurate sedimentation rate calculations as well as more detailed age-depth models.

Site U1314

Site U1314 (proposed Site GAR1B) is located on the southern Gardar Drift in a water depth of 2800 m (Fig. **F1**). Close to the location of Site U1314, a 33 m *Marion Dufresne* core (MD99-2253) was collected on the crest of the Gardar Drift in 1999. The MD99-2253 piston core has a high sedimentation rate of ~9 cm/k.y. for the last glacial cycle and well-defined planktonic $\delta^{18}O$ and geomagnetic paleointensity records. During Leg 162, Sites 983 and 984 were drilled off Iceland on the northern part of the Gardar and Bjorn Drifts, respectively (Fig. **F2**). These sites have mean Pleistocene sedimentation rates in the 10–15 cm/k.y. range and have produced high-resolution climatic and geomagnetic records. Sites 983 and 984, however, are located outside the main IRD belt (Fig. **F2**) and do not contain a robust detrital carbonate (Heinrich layer) signal. Furthermore, both sites are at shallower water depths (<2000 m) than Site U1314 and therefore monitor intermediate water but not NADW. Site U1314, on the other hand, is located (1) close enough to the IRD belt to record the Heinrich-type detrital layers that monitor ice sheet instability and (2) in a water depth of 2820 m, allowing a high-resolution monitoring of NADW and its short-term (sub)millennial variability.

Three holes (Holes U1314A, U1314B, and U1314C) were cored with the APC system and nonmagnetic core barrels to maximum depths of 258.4, 279.5, and 207.7 mbsf, respectively (Fig. **F9**). The average recovery was 102.7%. Drillover technique was not required for any of the three holes.

The sedimentary sequence at Site U1314 mainly consists of nannofossil- and clay-rich sediments with minor and varying proportions of diatoms and foraminifers. Only one lithologic unit was defined at Site U1314, which spans from the Late Pliocene to the Holocene (Fig. **F4**). In particular, two sets of lithologies can be identified: (1) predominantly nannofossil oozes enriched in biogenic (mainly diatoms and foraminifers) and terrigenous (principally clay minerals, quartz, opaque minerals, and calcite) components and (2) terrigenous silty clay with varying proportions of calcareous and siliceous organisms (Fig. **F4**). The sediment varies in color from very dark gray to light gray to hues of greenish gray. Slight to moderate bioturbation is typical for most of the section. Horizontal and parallel bedding planes and color contacts without erosional relief suggest that there is not visible evidence of significant sediment disturbance by natural processes. Sand- and gravel-sized sediment, common at Site U1314 from 0 to 240 mbsf, provides direct evidence of ice rafting and documents the influence of Pliocene–Pleistocene glaciations in this region. Based on the occurrence of

mafic igneous and felsic igneous dropstones, as well as sand-sized, hematite-stained quartz, Iceland and Greenland are probable source areas of the IRD material.

Site U1314 yields abundant assemblages of calcareous and siliceous microfossils spanning the Late Pliocene to the Holocene (Table **T1**). Sedimentation rates based on microfossil datums and paleomagnetism indicate decreasing rates from ~11–11.5 cm/k.y. during the Late Pliocene to ~7.0–7.5 cm/k.y. during the Pleistocene (Fig. **F5**). Polar and subpolar species dominate the assemblages, with subordinate amounts of transitional species present as well.

Calcareous nannofossils are abundant and generally well preserved throughout the section. Minor amounts of Cretaceous and Paleogene reworked nannofossils occur in all holes. Samples with increased amounts of reworked material typically contain coarser sediment and reduced abundances of in situ nannofossils. Late Pliocene discoasters are rare but present and can be used biostratigraphically, even though they are considered warm-water species. Generally well preserved planktonic foraminifers are the dominant component in the sand fraction of most core catcher samples, with lower proportions of benthic foraminifers, ostracodes, siliceous microfossils, and IRD. The fauna consists of species typical for transitional to subpolar provinces in the Pleistocene and Pliocene. *Neogloboquadrina pachyderma* (sinistral) is dominant in several of the glacial samples.

Radiolarians at this site show a great variation in species and abundances among the three holes. The state of preservation is generally good in all holes. *C. davisiana* is found in most samples, with a first common occurrence in Samples 306-U1314A-25H-CC and 306-U1314B-24H-CC. This species has a first common abundance in the North Atlantic at ~2.6 Ma. *Cycladophora sakaii* is commonly found in Samples 306-U1314A-25H-CC and 306-U1314B-25H-CC. In the North Pacific, *C. sakaii* evolves into *C. davisiana* at ~2.6 Ma. This is the first documented occurrence of *C. sakaii* in the North Atlantic. The last occurrence of *Spongaster tetras?* (2.6 Ma) is found in Samples 306-U1314A-28H-CC and 306-U1314B-27H-CC.

Abundant and diverse boreal to subarctic diatom flora, with a minor input of warm-water species, are present in all holes. The exception is the interval around Samples 306-U1314A-13H-CC to 15H-CC, where few or rare diatoms coincide with high content of siliciclastic material. The preservation is generally moderate to good, with a deteriorating trend downhole, as well as poor preservation coinciding with lithic-rich

intervals. The flora is dominated by long pennate specimens, as well as resting spores of *Chaetoceros* and fragments of big *Coscinodiscus* species.

The magnetostratigraphy at Site U1314 was constructed on the basis of continuous NRM measurements after AF demagnetization at a peak field of 20 mT. NRM intensities after 20 mT AF demagnetization are in the range of 10^{-1} to 10^{-2} A/m. These values are considerably greater than at Sites U1312 and U1313, owing to a higher magnetic mineral content. Site U1314 provides a very good record of the Brunhes, Matuyama, and the upper part of the Gauss (Fig. **F6**). The Brunhes/Matuyama reversal occurs at 57.3 ± 0.1 mbsf in Hole U1314A, 56.6 ± 0.1 mbsf in Hole U1314B, and 57.7 ± 0.1 mbsf in Hole U1314C. The deepest magnetic polarity interval recorded at Site U1314 corresponds to the top normal interval of the Gauss (Subchron 2An.1n; 2.58 Ma). Several short geomagnetic intervals are present in the paleomagnetic record, such as the Cobb Mountain and Reunion events. The magnetostratigraphy is consistent with the biostratigraphy throughout the section.

Stratigraphic correlation was straightforward at Site U1314 because most of the sediment physical properties show prominent short-wavelength amplitude variations related to changes in lithology. We relied mainly on between-hole correlation of distinctive magnetic susceptibility and natural gamma ray variations for depth shifting the cores. These correlations were confirmed to be consistent with geomagnetic polarity reversals recorded in the paleomagnetic inclination. The resulting mcd scale is well resolved, and the spliced section is complete down to 281 mcd. Because of core disturbance in the upper part of Hole U1314A, the splice in the interval 0–188.30 mcd was built from Holes U1314B and U1314C, with the exception of a short interval (65.80–69.50 mcd) where an undisturbed section of Core 306-U1314A-8H was incorporated into the composite section. From 188.30 to 300 mcd, the splice was constructed from Holes U1314A and U1314B because Hole U1314C was only drilled to 222 mcd. The two deepest cores (306-U1314B-29H and 30H), which span an interval not cored in Holes U1314A or U1314C, were appended to the splice. A growth factor of 1.08 is calculated by linear regression for the three holes at Site U1314, indicating an 8% increase in mcd relative to mbsf.

The ionic composition of the pore waters at Site U1314 was measured between Cores 306-U1314A-1H and 12H. Pore water alkalinity increases downhole from 5.34 to 7.46 mM. Ca^{2+} and Mg^{2+} concentrations decrease downhole from 8.4 to 5.2 mM and 48.7 to 37.4 mM, respectively. Fe^{2+} concentrations are variable with the lowest value (6.5 µM) measured at 36.4 mbsf, which coincides with more abundant darker lithologies.

Ba^{2+} concentration is higher at Site U1314 than at the IRD sites, ranging from 17 to 18.3 µM. Mn^{2+} concentration ranges from 46.8 to 15.9 µM and shows a rapid decrease downhole between 17.4 and 36 mbsf. H_4SiO_4 concentration increases with depth from 487.6 to 571.9 µM.

Carbonate concentrations in the sediments of Hole U1314A range from 3.7 to 70.5 wt%. The average carbonate value linearly shifts from 20 wt% at 250 mbsf toward 40 wt% near the top. $CaCO_3$ values show a good correlation to L* data throughout the section. TOC varies between <0.1 and 0.5 wt% (average = 0.2 wt%). The downhole TOC variation is similar to the variability in magnetic susceptibility, suggesting that organic carbon at Site U1314 is primarily of terrigenous origin. Based on initial results from eight samples, solvent-extractable organic matter at Site U1314 consists mainly of long-chain, odd-numbered C_{25}–C_{35} *n*-alkanes and long-chain C_{37}–C_{40} alkenones. Except for one sample from the Late Pliocene, all Pleistocene samples show a distinct prevalence of *n*-alkanes relative to alkenones, confirming the assumption of a mainly terrigenous origin of the organic matter at Site U1314. Alkenone-derived SSTs vary between ~10° and 13°C.

Physical property measurements at Site U1314 included nondestructive measurements of magnetic susceptibility, density, *P*-wave velocity, and natural gamma radiation (Fig. **F9**). Working sections were used to measure MAD and compressional *P*-wave velocity. These properties are positively correlated consistent with the terrigenous nature of the sediment. The magnetic susceptibility records, for example, show a highly variable record attributed to lithologic and/or mineralogic changes; multiple excursions toward high values are generally associated with IRD layers.

At Site U1314, a complete Upper Pliocene to Holocene sequence, characterized by high sedimentation rates of 7 to >11 cm/k.y., was recovered. Because of its location close to the IRD belt and within NADW, as well as its high potential for paleomagnetic and isotopic age control, this section will be used to establish a high-resolution (millennial to submillennial) environmental record of sea-surface and bottom water characteristics and a detrital (Heinrich type) stratigraphy for the past ~2.7 m.y.

Site U1315

Site 642, located on the Vøring Plateau in a water depth of ~1280 m, was first drilled during ODP Leg 104 (Eldholm, Thiede, Taylor, et al., 1987). In Hole 642E, a 1229 m deep sequence was drilled that is composed of upper Eocene to Quaternary biogenic

and terrigenous sediments with volcaniclastics in the lower part (Units I to IV; 0–315 mbsf) and Eocene tholeiitic (upper series) and andesitic (lower series) basalt flows with interbedded volcaniclastic sediments (315–1229 mbsf). The location of Site 642 was revisited during Expedition 306 (Site U1315A; 67°12.74′ N, 02°56.24′ E).

The primary objective at this site is to document bottom water temperature variations and monitor subbottom diffusion over a 5 y period. Bottom water temperature and salinity variations are monitored with instruments that sit in the water column by way of an elevated reentry cone. Diffusion of the thermal wave through the subsurface is monitored with a 150 m thermistor string deployed in a cased and CORKed borehole. Hole U1315A was drilled to a depth of 179.07 mbsf and cased with $10^3/_4$ inch casing. The base of the casing was cemented, and the casing string was displaced with bentonite mud. The thermistor string is attached to Spectra rope using friction tape, cable ties, and marine duct tape to carry the weight of the load and the 250 lb sinker bar. The thermistor string is connected to a data logger and external battery at the top.

Downhole Logging of Hole 642E

To assess current background thermal conditions in the region, a downhole record of temperature from nearby Hole 642E was obtained using the LDEO Temperature/Acceleration/Pressure (TAP) tool in combination with the triple combo. In addition, the FMS-sonic tool string was deployed. At a depth of 588 mbsf, an impassable obstruction was reached and downhole logging had to be stopped. The TAP tool indicated a bottom water temperature at the seafloor of ~0.2°C. The upper 10 m of the borehole had a very steep gradient (~2500°C/km). Below this depth, the borehole had a relative low gradient of ~22°C/km. At a depth of ~500 mbsf, a strong positive temperature excursion to ~42°C may indicate inflow. FMS imaging of the hole yielded good results and will allow the correlation to existing core data and filling in the gaps (~60% of the formation). In combination with detailed FMS resistivity measurements and imaging and sonic data, it will be possible to obtain reliable permeability estimates. Understanding the permeability will allow better understanding of fluid flow and temperature gradients observed in the borehole.

Parts A and B Summary

DISCUSSION AND CONCLUSIONS

Following Expedition 303, Expedition 306 was the second cruise of the North Atlantic climate study that aims to generate a late Neogene–Quaternary chronostratigraphic template for North Atlantic climate proxies that can be correlated at a sub-Milankovitch scale and exported to other parts of the globe by using a PAC. In addition, Expedition 306 also included the installation of a CORK near Site 642 (Vøring Plateau, Norwegian margin) to investigate the feasibility of reconstructing bottom water temperature histories at the decade to centennial timescale by making high-precision temperature-depth measurements.

Based on the Expeditions 303 and 306 *Scientific Prospectus* and the results of Expedition 303, proposed Sites IRD3A and IRD4A and two sites on Eirik Drift were originally selected to become the primary Expedition 306 sites. Extremely bad weather conditions in the Labrador Sea, however, did not allow coring operations on Eirik Drift at any time. Thus, we concentrated our work related to the North Atlantic paleoceanography study in the area directly south of the central North Atlantic IRD belt and on the southern Gardar Drift. These locations are known either from Leg 94 or from conventional piston coring to have the potential for paleomagnetic and isotopic age control and sedimentation rates high enough for high-resolution reconstructions of sea-surface and bottom water characteristics and ice sheet instabilities during late Neogene to Pleistocene times.

The main objective at Site U1312, a reoccupation of Site 608, was to obtain continuous records of surface and deepwater characteristics and their interactions with ice sheet instabilities during Neogene–Quaternary times. In this context, an important target at this site was the recovery of a complete undisturbed upper Miocene section by means of APC coring. The Holocene to upper Miocene sedimentary succession at Site U1312 consists of varying mixtures of biogenic and detrital components, primarily nannofossils, foraminifers, and clay minerals. At ~3.5 Ma, the progressive but oscillatory deterioration of the northern hemisphere climate, which gradually led to the onset of major continental ice sheets at ~2.7 Ma, is reflected in the increase in detrital sediment input, followed by Late Pliocene–Pleistocene climate-controlled short-term variability in detrital input. Average sedimentation rates were low during the late Miocene and in the latest Pliocene and Pleistocene (1–2 cm/k.y.) and higher in the Early Pliocene (3–8 cm/k.y.).

- *The sedimentary sequence of Site U1312 representing the last ~11 m.y. will allow the study of short- and long-term climate variability and ocean/atmosphere interactions under very different boundary conditions, such as the closure and reopening of Atlantic/Mediterranean connections at the end of the Miocene (6–5 Ma), the closing of the Isthmus of Panama (4.5–3 Ma), and the onset of major northern hemisphere glaciation near 2.7 Ma.*

Site U1313 is a reoccupation of Site 607. Site 607 has been very important for generating a Late Pliocene to Pleistocene stable isotope stratigraphy that can be interpreted in terms of ice sheet variability and changes in NADW circulation. At the site of Core VM 30-97, located close to Site 607, Heinrich events are marked by the distinctive detrital carbonate signature, and planktonic-foraminifer-derived SSTs warmed markedly during the Heinrich events and during the Last Glacial Maximum, in distinct contrast to the climate records from the subpolar North Atlantic.

At Site U1313, four holes with a maximum penetration to 308.6 mbsf were drilled. The Holocene to uppermost Miocene sedimentary succession at Site U1313 consists primarily of nannofossil ooze with varying amounts of foraminifers and clay- to gravel-sized terrigenous components. The detrital components become much more important and variable in the Upper Pliocene–Pleistocene interval of the sequence, probably reflecting northern hemisphere ice sheet instability. Bio- and magnetostratigraphy indicate nearly constant sedimentation rates of ~4.1–4.5 cm/k.y. throughout the Pliocene–Pleistocene time interval, whereas in the late Messinian, sedimentation rates were ~13–14 cm/k.y. Correlation between the holes was excellent in the upper 168.5 mcd because of pronounced variations in nearly all physical properties measured. In particular, L* from color reflectance measurements mimic variations in the global benthic oxygen isotope stack (e.g., Lisiecki and Raymo, 2005), and a preliminary age model was constructed by matching sharp L* variations with glacial and interglacial terminations. Alkenone-derived SSTs show variability from ~13° to 19°C during the Pleistocene, whereas temperatures of ~20° and 22°C are obtained for the Late Pliocene and the latest Miocene, respectively. The consistency of downhole logging data with both core data and age models will allow mapping of the spliced core record to actual depth, resulting in more accurate sedimentation rate calculations as well as more detailed age-depth models. Of special note is the dramatically consistent linear correlation of downhole natural gamma radiation (upper 225 mbsf) with the recent Lisiecki and Raymo (2005) benthic oxygen isotope record during the last 5.4 m.y.

- *Site U1313 provides a unique and complete Pliocene–Pleistocene sediment section with remarkably constant sedimentation rates. This site will allow an optimal reconstruction of the phasing of the temperature records and its relationship to ice sheet instability and changes in deepwater circulation throughout the last 5 m.y. High sedimentation rates of 13–14 cm/k.y. will allow a high-resolution study of paleoenvironmental change during the late Messinian.*

Site U1314 was drilled on the southern Gardar Drift, close enough to the IRD belt to record Heinrich-type detrital layers that monitor ice sheet instability, at a water depth of 2800 m, allowing a high-resolution monitoring of NADW and its short-term (sub)millennial variability.

The Upper Pliocene to Holocene sedimentary sequence at Site U1314 consists of an alternation of predominantly nannofossil oozes enriched in biogenic and terrigenous components and terrigenous silty clay with varying proportions of calcareous and siliceous organisms. This alternation is also reflected in the carbonate content varying between ~5 and 70 wt%. Sand- and gravel-sized sediment, common at Site U1314 from 0 to 240 mbsf, provides direct evidence of ice rafting and documents the influence of Pliocene–Pleistocene glaciations on this region. Site U1314 yields abundant moderately well to well-preserved assemblages of calcareous and siliceous microfossils throughout the section and an excellent paleomagnetic record of the Brunhes, Matuyama, and the upper part of the Gauss Chrons. Even several short geomagnetic reversals are present in the paleomagnetic record. Sedimentation rates based on microfossil datums and paleomagnetic reversals indicate decreasing rates from ~11–11.5 cm/k.y. during the Late Pliocene to ~7.0–7.5 cm/k.y. during the Pleistocene. Stratigraphic correlation was straightforward at Site U1314 because most of the sediment physical properties show prominent short-wavelength amplitude variations. The resulting mcd scale is well resolved, and the spliced section is complete down to 281 mcd.

- *At Site U1314, a complete Upper Pliocene to Holocene sequence, characterized by high sedimentation rates of 7 to >11 cm/k.y., was recovered. Because of its location close to the IRD belt and within NADW, this section will be used to establish a high-resolution (millennial to submillennial) environmental record of sea-surface and bottom water characteristics and a detrital (Heinrich type) stratigraphy for the past ~2.7 m.y.*

At Site U1315, a borehole observatory consisting of a CORK to seal the borehole from the overlying ocean and a thermistor string/data logger unit to document BWT variations and monitor its subbottom diffusion over a 5 y period, was successfully installed in a new hole ~180 m deep, close to Site 642. To assess current background

thermal conditions in the region, logging down to almost 600 mbsf was performed in Hole 642E using the TAP tool in combination with the triple combo and the FMS-sonic tool strings. The upper 10 m of the borehole has a very steep thermal gradient (~2500°C/km). Below this depth, the borehole has a relative low gradient of ~22°C/km. At a depth of ~500 mbsf, a strong positive temperature excursion to ~42°C may indicate inflow.

From the multidisciplinary (i.e., sedimentological, micropaleontological, and geochemical) studies to be performed on these cores (together with cores from Expedition 303) in the coming years, new milestones in the understanding of mechanisms and causes of abrupt climate change as one of the major challenges in global climate change research today are expected to be reached.

The success of our expedition was substantially supported by the excellent cooperation between the IODP staff, the Transocean employees, and the Shipboard Science Party, and the strong efforts of all of them.

PRELIMINARY SCIENTIFIC ASSESSMENT

IODP Expedition 306 was based on two separate proposals titled (A) "Ice sheet–ocean atmosphere interactions on millennial timescales during the late Neogene–Quaternary using a paleointensity-assisted chronology for the North Atlantic" and (B) "Installation of a CORK near Hole 642E to document and monitor bottom water temperature variations through time." Following Expedition 303, Expedition 306 was the second cruise of the North Atlantic paleoceanography study that aimed to generate a late Neogene–Quaternary chronostratigraphic template for North Atlantic climate proxies and allowed their correlation at a sub-Milankovitch scale and their export to other parts of the globe by using a PAC.

Based on the Expeditions 303 and 306 *Scientific Prospectus* and the results of Expedition 303, Sites IRD3A and IRD4A and two sites on Eirik Drift were selected to become the primary Expedition 306 sites. Continuous weather observations performed throughout Expedition 306 showed, however, that coring operations on Eirik Drift were not possible at any time because of extremely bad weather conditions in the Labrador Sea. Thus, the alternate Site GAR1B was elevated to a primary site instead. In total, we lost 10 days because of severe weather conditions in the first part of the expedition. Therefore, only three sites (Sites U1312 [IRD4A], U1313 [IRD3A], and U1314 [GAR1B]) could be drilled instead of the planned four sites. However, Expedition 306

was completed successfully and the objectives outlined in the 303/306 *Scientific Prospectus* and *Addendum* were fulfilled:

- For the North Atlantic paleoceanography study, we recovered complete sedimentary sections at three sites. The excellent sections from Sites U1313 and U1314 provide the requirements, including adequate sedimentation rates, to study millennial-scale environmental variability in terms of ice sheet-ocean interactions, deep circulation changes, or sea-surface conditions. Site U1313 provides a unique and complete Pliocene–Pleistocene sediment section with remarkably constant sedimentation rates. This site will allow for an optimal reconstruction of the phasing of temperature records and their relationship to ice sheet instability and changes in deepwater circulation throughout the last 5 m.y. High sedimentation rates of 13–14 cm/k.y. will allow a high-resolution study of paleoenvironmental change during the late Messinian. At Site U1312, unfortunately, only two holes could be drilled because of severe weather conditions. Although the recovery in these holes was very good, a complete splice could only be obtained between 68 and 159 mcd. The upper 68 mcd of Hole U1312A was affected by coring disturbance. Below 159 mcd, both holes are of high quality but splicing the two records was not possible because of a very uniform sediment composition. Furthermore, at this site, sedimentation rates are quite low, especially in the late Miocene, the major target at Site U1312 (<1–2 cm/k.y.). Thus, high-resolution studies could not be performed at this site. The almost-complete sedimentary sequence from Site U1312 representing the last ~11 m.y., however, will allow the study of short- and long-term climate variability and ocean-atmosphere interactions under very different boundary conditions, as outlined in the previous sections.
- Our second Expedition 306 main target was the CORK program. Here, a borehole observatory with a 150 m thermistor string was successfully deployed in a cased and CORKed borehole close to Site 642. The data recovered in the coming years will provide for the first time a directly measured record of BWT over approximately the last 100 y from a paleoceanographically very important key area of the North Atlantic.

Because two of the 306 sites (U1312 and U1313) are redrillings of Sites 607 and 608, expectations of the type and age of sediments existed prior to the 306 drilling. At the third Site U1314, information about the sedimentary type and sedimentation rates/age had been obtained for the upper 30 m from a *Marion Dufresne* piston core. In this context, the material recovered met expectations.

Besides the coring and CORK activities, the downhole logging at Sites U1313 and in Hole 645E was extremely useful and another highlight of the expedition. An excellent correlation between downhole logging and shipboard MST logging was possible. This allows, for example, calculation of "real" sedimentation rate values. In Hole 645E, FMS logging yielded very good results and allows correlation to existing core data and filling of coring gaps (60% of the formation!). Together with the other downhole logging data, detailed information about permeability, fluid flows, and temperature gradients of the area will be available.

Looking back at the process of the expedition and the evolution of the weather conditions, we have to mention that early spring (March) was not the right season to perform drilling operations in the North Atlantic. During the second part of the expedition, we had optimum weather conditions for conducting the CORK program very successfully. The CORK working area, however, was very far away from our main working area of the North Atlantic Paleoceanography program (i.e., >5 days of transit). Here, it would have been useful to have the approval for an alternative coring program close to the CORK area in advance. If weather conditions would have been too severe to conduct the CORK program, we had no real alternative program at that time.

Some of the drill sites proposed in the original proposal (572-Full3) and the *Expeditions 303 and 306 Addendum* could not be drilled during Expeditions 303 and 306, respectively: Sites IRM2A and IRM3A (revisiting the area of ODP Sites 918 and 919) (Larsen, Saunders, Clift, et al., 1994) were already skipped prior to the expeditions because of weather windows, and the high-priority LAB8 sites could not be drilled during Expedition 306 because of severe weather conditions during the campaign. These sites should be considered in future drilling expeditions in the North Atlantic to complete the "Ice sheet-ocean-atmosphere interactions on millennial timescales during the late Neogene–Quaternary" objectives.

The IRM3A and IRM2A sites—located in the Irminger Basin on the path of the East Greenland Current and deep waters resulting from Denmark Strait overflow, the major component of NADW—are sensitive to millennial-scale instabilities of coastal ice sheets of the East Greenland/Icelandic area and are influenced by instabilities of the Laurentide Ice Sheet. Drilling results from some of the LAB8 transect sites could extend the climate record back into the Miocene and answer questions about the sedimentary architecture of sediment drifts, the role of the Western Boundary Under-

Current (WBUC) in NADW formation, and provide a unique record of Greenland Ice Sheet instability.

In a future drilling campaign related to the "Ice sheet-ocean-atmosphere interactions on millennial timescales during the late Neogene–Quaternary," it might also be useful to consider drill sites strongly influenced by IRD input from the British-Fennoscandian Ice Sheet. Here, potential candidates could be DSDP Site 548, drilled southwest of Ireland across the continent/ocean boundary on the sediment-starved Goban Spur (De Graciansky, Poag, et al., 1985), and ODP Site 644 located on the Vøring Plateau (Eldholm, Thiede, Taylor, et al., 1987). A comparison between records from Sites U1305–U1307 (western "end-member" proximal to the Laurentide/Greenland Ice Sheet), Sites IRM3A and IRM2A ("end-member" of coastal ice sheets of the East Greenland/Icelandic area), Sites U1304 and U1308 (central part of the IRD belt), and new sites at the location of DSDP Site 548 (eastern "end-member" proximal to the British Ice Sheet) and ODP Site 644 ("end-member" proximal to the Fennoscandian Ice Sheet) (see Fronval et al., 1997) will allow a high-resolution (millennial to submillennial) reconstruction of the (contemporaneous and/or nontemporaneous) history of the Laurentide, Greenland, and British-Fennoscandian ice sheets' instability and their relationship to surface water and deepwater characteristics.

OPERATIONS

Port Call

Expedition 306 officially began with the first line ashore on Ponta Delgada, Azores (Portugal), at 1805 h on 2 March 2005. The third Ponta Delgada port call in a row for the *JOIDES Resolution*, which included refueling and restocking bentonite and attapulgite bulk drilling mud, was concluded at 0806 h on 9 March, ~1.8 days behind schedule because of problems with the passive heave compensator (PHC) seal replacement and severe weather that significantly hampered (and slowed) the PHC repair work. Jeff Fox, Director, Science Services, IODP-Texas A&M University (TAMU), attended the port call accompanied by the new TAMU Dean of Geosciences, Dr. Bjorn Kjerfve. We completed the transit from Ponta Delgada to Site U1312 averaging 10.3 kt over the 344 nmi distance.

Site U1312

Hole U1312A

We arrived at Site U1312 (proposed Site IRD4A) at 1730 h on 10 March and spudded Hole U1312A at 0830 h on 11 March. Core 1H was recovered in full (10.08 m), suggesting a seafloor depth of 3533.0 mbsf (Table **T2**). Because of excessive heave (≥5 m), initial coring conditions were not optimal and a more realistic seafloor depth estimate was obtained later in Hole U1312B. APC coring, utilizing nonmagnetic core barrels, continued to a depth of 237.5 mbsf. The first several cores (1H through 10H to 95.0 mbsf) had questionable shear pressures, and Core 1H required two wireline runs to recover because of a sheared overshot pin. The swell height decreased after Core 10H, and coring system performance improved accordingly. Coring in Hole U1312A was terminated after recovering Core 25H. The drillover technique was required for recovery of Cores 23H through 25H, and all core barrels fully stroked. Drillover for the last core required 2 h in the semi-indurated white ooze, and Core 23H was recovered bent. Coring may have continued further; however, the risk to the equipment was significant, the time required for further advancement was reaching a diminishing return, and the co-chief scientists were concerned about getting Hole U1312B initiated while heave conditions remained low (~1.5 m). In Hole U1312A, we cored 237.5 m, recovering 248.07 m (104.45%).

Hole U1312B

After the seafloor was cleared, the vessel was offset 25 m to the northwest of Hole U1312. Hole U1312B was spudded at 2115 h on 12 March, with the bit positioned at a depth of 3528.0 mbsf, 5.0 m higher than at Hole U1312A. Core barrel 1H advanced 9.5 m and recovered 3.92 m of sediment, placing the seafloor depth for Hole U1312B at 3533.6 mbsf. After successfully achieving a good mudline core, piston coring advanced to 231.9 mbsf. The core line failed at the rope socket while attempting to recover Core 18H, necessitating a wireline fishing trip for the core barrel and sinker bar assembly. Coring continued through Core 25H (231.9 mbsf) as weather conditions progressively deteriorated, leading to another damaged core line at the rope socket and twisted piston rods. Before repairs were completed, weather conditions deteriorated to a point that precluded additional coring. A wind shift and increased velocity forced a heading change to maintain position over the hole. This caused excessive roll as the ship was exposed to multiple large swells coming from different directions. Because the electrical supervisor expressed concern about the ability to keep the ship on location, the drill string was pulled out of the hole, clearing the seafloor at 0245 h on

14 March. The ship was allowed to drift off location to minimize vessel motion during the remainder of the pipe trip. By 1700 h on 14 March, the ship was secured and began the slow dynamic positioning move into the prevailing seas back over the drill site. At 0430 h on 15 March positioning beacon SN 2199 (15 kHz, 211 dB) was recovered, officially ending operations for Hole U1312B and Site U1312. In Hole U1312B, we cored 231.9 m, recovering 236.84 m (102.08%).

Transit to Site U1313

We departed the Azores Islands for Site U1313 (proposed Site IRD3A) at 0645 h on Saturday, 26 March, after spending 8 days in the lee of the islands from severe weather conditions. The 277 nmi transit to Site U1313 began with sea-state conditions still somewhat marginal but expected to continuously improve over time. The transit was completed at an average speed of 8.9 kt, and we arrived at Site U1313 at 1425 h on Easter Sunday, 27 March.

Site U1313

Hole U1313A

Hole U1313A was spudded at 0005 h on 28 March, establishing a rig floor-corrected seafloor depth of 3423.3 meters below rig floor (mbrf). Core 1H recovered 5.2 m of sediment, indicating a seafloor depth of 3412.3 mbsl. APC coring, utilizing nonmagnetic core barrels, continued through Core 31H. Alloy steel barrels were utilized for Cores 32H and 33H, and drillover of stuck APC barrels was required for these last two cores. Tensor core orientation was used for all cores beginning with Core 3H from a depth of 14.7 mbsf. All core barrels fully stroked except for the last one, Core 33H. The cored interval for this hole was 308.6 m, and 319.64 m of sediment was recovered (103.6%). The drill string was pulled clear of the seafloor at 1300 h on 29 March, concluding operations in Hole U1313A.

Hole U1313B

Hole U1313B was offset 25 m due north (000°) from Hole U1313A and was spudded at 1430 h on 29 March. The bit was positioned at a depth of 3421.0 mbrf, or 2.0 m deeper than Hole U1313A, and Core 1H recovered 5.90 m of sediment, establishing a rig floor-corrected seafloor depth of 3424.6 mbrf. APC coring continued through Core 20H to a depth of 186.4 mbsf. At that time, operations personnel were advised that the core breaks between Holes U1313A and U1313B were possibly becoming aligned.

As a precaution to ensure adequate overlap between holes, the driller was advised to advance the bit 2.0 m further before shooting Core 21H. Coring then continued until 1930 h on 30 March, through Core 32H to a total depth of 302.4 mbsf. Tensor core orientation was used for all cores beginning with Core 3H from a depth of 15.4 mbsf. All core barrels fully stroked, and no drillover was required in this hole. Nonmagnetic core barrels were used in the recovery of all 32 cores. The cored interval for this hole was 300.4 m, and 306.54 m was recovered (102.0%).

After completing coring operations, Hole U1313B was prepared for logging. A wiper trip was conducted from total depth to 74.9 mbrf and back to total depth without difficulty. No fill, drag, or overpull was detected. The hole was swept with one final 30 bbl mud sweep, and the lockable float valve (LFV) go-devil was pumped down to lock open the LFV for the wireline logging tools. The hole was displaced with 140 bbl of sepiolite mud, and the drill pipe was retracted to 80.7 mbsf. The triple combo tool string was deployed (including the GPIT and MGT tools) to within 2.0 m of the bottom of the hole. We successfully logged 220 m of the open hole and then the interval within the pipe to the seafloor. The scheduled deployment of the FMS-sonic tool string was cancelled because the LDEO Logging Staff Scientist felt that the resistivity signal was too weak to make the deployment worthwhile. After recovery of the wireline tools, new software for the Schlumberger wireline heave-compensated logging winch was briefly tested. The software was tested for ~45 min under a variety of conditions, and the results appeared to be “very promising.” The Schlumberger logging sheaves were rigged down, and the drill string was pulled clear of the seafloor at 1310 h on 31 March, ending Hole U1313B.

Hole U1313C

The drillship was offset 25 m due east (90°) of Hole U1313B. The bit was positioned at a depth of 3417.0 mbrf, or 2.0 m shallower than for Hole U1313A. Hole U1313C was spudded at 1440 h on 31 March. Core 1H recovered 2.71 m and established a rig floor-corrected seafloor depth of 3423.8 mbrf. APC coring with nonmagnetic core barrels continued through Core 30H, and alloy steel barrels were used for the last two cores (31H and 32H). Tensor core orientation was used for all cores beginning with Core 4H from a depth of 21.7 mbsf. Drillover was required for recovery of Cores 29H through 32H. All core barrels fully stroked except for the last three (Cores 30H through 32H). The bit was advanced by 8.73 m prior to shooting Core 32H. The drill string was pulled clear of the seafloor at 2140 h on 1 April, officially ending Hole

U1313C. The cored interval for this hole was 293.4 m, and 305.79 m of sediment was recovered (104.2%).

Hole U1313D

The drillship was offset 25 m due south (180°) of Hole U1313C. The bit was positioned at a depth of 3423.0 mbrf, or 4.0 m deeper than for Hole U1313A. Hole U1313D was spudded at 2255 h on 1 April. Core 1H was recovered in full (9.80 m); therefore, the seafloor depth of 3423.0 mbrf was considered suspect. A valid seafloor depth was not critical for this hole because three good seafloor measurements had already been obtained on the three previous holes and the emphasis was to maximize recovery in Core 1H. APC coring continued without incident in Hole U1313D through Core 16H to a total depth of 152.0 mbsf. Tensor core orientation was used for all cores, beginning with Core 3H from a depth of 19.0 mbsf. All core barrels fully stroked, and no drillover was required. Nonmagnetic core barrels were used for recovery of all 16 cores. The cored interval for this hole was 152.0 m, and 159.27 m of sediment was recovered (104.8%).

The drill string was pulled clear of the seafloor at 1310 h on 2 April, and, during the pipe trip positioning, beacon SN 2199 was recovered at 1430 h. After we recovered and stored the drill string, the ship was secured for transit, all thrusters and hydrophones were pulled, and at 2030 h, the ship was switched from dynamic positioning to cruise mode and got under way for alternate Site U1314 (proposed Site GAR1B).

Transit to Site U1314

We arrived at Site U1314 (proposed Site GAR1B) early Thursday morning, 7 April, after a 943 nmi transit from Site U1313. Positioning beacon SN 2199 (15.0 kHz, 211 dB) was deployed at 0330 h, and operations at Site U1314 officially began.

Site U1314

Hole U1314A

Hole U1314A was spudded at 0950 h on 7 April. Core 1H recovered 1.95 m of sediment and established a rig floor-corrected seafloor depth of 2810.6 mbrf. APC coring continued without incident in Hole U1314A until Core 28H at a depth of 258.4 mbsf. The overshot pin sheared during the attempt to recover Core 28H. Unfortunately, the driller did not initially realize that the core barrel was not being recovered and proceeded to drill downhole in preparation for the next core. After recovering the core

barrel on the second wireline run, the APC system was found to be heavily damaged, including overtorqued piston rod connections and other damage. Because it was going to take an hour or more to repair and rebuild the APC system, the co-chief scientists elected to terminate coring in Hole U1314A and proceed with the next hole. After repairing the APC, the drill string was pulled clear of the seafloor at 1100 h on 8 April, officially ending Hole U1314A.

Tensor core orientation was used for all cores beginning with Core 4H from a depth of 20.9 mbsf. Drillover of stuck APC barrels was not required, and all core barrels fully stroked. Nonmagnetic core barrels were used to recover all 28 cores. Problems with swollen or imploded core liners were more prevalent in this hole than experienced previously at the other sites. Of 28 cores recovered, 4 liners suffered some swelling (Cores 12H, 15H, 16H, and 23H) and 6 core liners either shattered (Core 20H) or imploded (Cores 18H, 22H, 26H, 27H, and 28H). In addition, four barrels mechanically sheared during deployment (Cores 2H, 4H, 6H, and 11H). These problems were most likely heave induced and led to more disturbed and lower-quality core than normally experienced with the APC system. The cored interval for this hole was 258.4 m, and 267.34 m of sediment was recovered (103.5%).

Hole U1314B

The drillship was offset 25 m due north (000°) of Hole U1314A. The bit was positioned at a depth of 2806.0 mbrf, or 3.0 m deeper than Hole U1313A, to offset the core breaks between cores. Hole U1314B was spudded at 1220 h on 8 April, and Core 1H recovered 4.02 m and established a rig floor-corrected seafloor depth of 2811.5 mbrf. APC coring with nonmagnetic core barrels continued without incident in Hole U1314B through Core 30H to a total depth of 279.5 mbsf. Tensor core orientation was used for all cores beginning with Core 4H from a depth of 23.0 mbsf. All core barrels fully stroked, and no drillover was required in this hole. The cored interval for this hole was 279.5 m, and 285.36 m of sediment was recovered (102.1%). The drill string was pulled clear of the seafloor at 1155 h on 9 April, officially ending Hole U1314B. Although there still were some core liner incidents at this hole, core quality was improved. Of the 30 cores recovered, 4 liners were recovered swollen (Cores 15H, 21H, 22H, and 26H) and another 3 were imploded at the bottom end (Cores 9H, 19H, and 27H). The overshot pin sheared once on Core 6H, requiring a second wireline run to recover the core barrel.

Hole U1314C

The drillship was offset 25 m due east (90°) of Hole U1314B. The bit was positioned at a depth of 2809.0 mbrf, or 6.0 m deeper than Hole U1314A, again to offset the core breaks between cores. Hole U1314C was spudded at 1320 h on 9 April, and Core 1H recovered 8.22 m and established a rig floor-corrected seafloor depth of 2810.3 mbrf. APC coring with nonmagnetic core barrels continued in Hole U1314C through Core 22H to a total depth of 207.7 mbsf. During this period, the weather deteriorated as a major gale approached our location and brought high winds and steadily building seas and swells with it. By Sunday morning, we had long-period heave cycles in excess of 5 m and storm-force winds were forecast for the Site U1314 location by late Sunday or early Monday. Tensor core orientation was used for all cores beginning with Core 3H from a depth of 17.7 mbsf. All core barrels fully stroked, and no drillover was required in this hole. The cored interval for this hole was 207.7 m, and 212.93 m of sediment was recovered (102.5%). The drill string was pulled clear of the seafloor at 0915 h on 10 April, and positioning beacon SN 2199 was recovered during the pipe trip, officially ending Site U1314 at 1030 h. After we recovered and stored the drill string, the ship was secured for transit and all thrusters and hydrophones were pulled. At 1545 h on 10 April, the ship was switched from dynamic positioning to cruise mode and began the sea voyage to Site U1315 (Site 642 in the Vøring Plateau).

Transit to Site U1315

We arrived at Site U1315 (proposed Site 642) on the morning of 15 April after a 1190 nmi transit from Site U1314. By 1120 h, the positioning beacon was deployed and operations at the site officially began.

Site U1315

Hole U1315A

After we verified the seafloor depth with the television/sonar system (1283.0 mbrf), the drill string was recovered back to the drillship and we prepared to assemble and deploy the “elevated” reentry cone assembly and $10^3/_4$ inch casing string. Following assembly, the drill string with the reentry cone structure, $10^3/_4$ inch casing, and the mud motor and underreamer drilling assembly were tripped to the seafloor, spudding Hole U1315A at 2130 h on 15 April. The base of the reentry cone reached the seafloor at 0515 h in the morning on 16 April, resulting in an average rate of penetration of

21.9 m/h. The drill string was released from the reentry cone/casing assembly at 0550 h and then recovered back to the ship.

The drill string was reassembled with a cementing bottom-hole assembly and reentry cleanout bit and tripped to the seafloor, and Hole U1315A was reentered at 2026 h on 17 April. A 5 bbl, 15.8 ppg cement plug was displaced to bottom. The pipe was pulled clear of the seafloor/reentry cone, and the vessel was offset 30 m south where the drill pipe was thoroughly circulated clean. After the cement set, we reentered the hole and lowered the pipe, tagging the top of the cement at ~164.2 mbsf or ~11.6 m above the casing shoe, which was within 1.6 m of our 10.0 m target height for the top of the cement column. After the casing string was displaced with bentonite mud, the drill string was retrieved in preparation for the CORK deployment in Hole U1315A.

CORK Deployment

The CORK running tool was made up to a 2.0 m drill collar pup joint and was laid out on the rig floor. The antitorsion ring, a recent modification that is designed to prevent accidental release of the tool during deployment, was installed along with the seal stinger. The Hole U1315A CORK head was moved from the core tech shop roof to the starboard side of the pipe stabber using the number 2 crane. From there, the load was transferred to two tugger lines and the head was placed through the rotary table with the bushings removed. The head was supported using $13^{3}/_{8}$ inch casing slips with a dog collar installed above. The running tool was picked up with the drawworks elevators and was easily installed on the CORK head.

Two stands of $8^{1}/_{4}$ inch drill collars were made up to the top of the running tool, and the CORK assembly was lowered to the seafloor. During the pipe trip, the subsea television/vibration-isolated television (VIT) frame was being lowered when the video was suddenly lost. The VIT was recovered, and troubleshooting identified a cleared power circuit breaker resulting from water leakage. In addition, a broken strand of outer armor was discovered ~360 m above the cable head termination. The resulting snarl in the armor was cut off, and the ends were secured. Once the cable head was on deck, we discovered that water had entered the oil-filled section of the cable head. The cable head connection was repaired rather than spending costly time completely reheading the cable. The VIT was ready to deploy once again at 0345 h on 19 April. A total of 3.25 h was required to make the necessary repairs.

Hole 1315A was reentered for the third and final time at 0448 h on 19 April. Space out was tight given the short length of the CORK stinger (20.85 m). For thermistor

string deployment, the CORK head was left 9.0 m shy of landing out in the 16 inch casing hanger. This left ~12.3 m of stinger in the hole and allowed the pipe to be hung off at the rotary table to break the drill pipe connection and deploy the thermistor string.

Thermistor String Deployment

A total of 5.75 h was required to make up and deploy the thermistor string. This string was specially designed for long-term monitoring of the upper 150 m of the sediment column from the seafloor down. The thermistor string was premade up with a $^1/_4$ inch diameter Spectra (Kevlar) rope attached to the thermistor cable with tie wraps and duct tape. The Spectra line (153.84 m) was designed to carry the load as a tension member and was terminated with a ~250 lb sinker bar (3.73 m). The thermistor cable was plugged into a battery pack/data logger assembly (0.97 m) at the top. This package was suspended from another short section of Spectra rope (2.22 m) with thimbles at each end and the XN latch assembly (0.31 m to landing shoulder). Cable "grips" were used to lift the thermistor string in ~50–60 ft lifts using a double sheave assembly and two tugger lines. This was the same process used on earlier thermistor deployments; however, this time, there were problems. For reasons yet to be fully understood, at the conclusion of each lift, the thermistor cable tensed up and carried the load and the Spectra line would go slack. On most lifts, the load would eventually transfer back to the Spectra line as designed; however, on the last two lifts, the load never did transfer. Fortunately the Hole U1315A thermistor string was relatively short, and the suspended load was fairly light. To rectify the problem, we cut loose the remaining tie wraps and duct tape. We then retied and retaped the cable and rope together as the remainder of the string was deployed. At the end, where the rope was to be attached to the bottom of the data logger/battery assembly, we had a surplus of 9 ft of Spectra rope that had to be cut off, leaving the final rope length at 151.10 m. Once made up, the thermistor string assembly was deployed via wireline at 1030 h on 19 April. The XN latch assembly was landed without incident. The latch was jarred down for setting, and a 4000 lb overpull was taken to verify proper latch-in. The sinker bars were recovered via wireline, and by 1215 h we were ready to land and release the CORK assembly.

CORK Landing and Release

The drill string was lowered the remaining 9.0 m (~1 knobby joint), and the CORK head landed out at exactly the correct pipe depth. About 5000 lb were put down, and then ~8000 lb of overpull was taken to verify that the CORK head was latched. This

weight was slacked off, and a small amount of right hand-torque was applied to the string. The CORK running tool was visually observed to rotate slightly, and when the string was picked up, the running tool lifted cleanly off the head. Installation of the Hole U1315A CORK was officially completed as of 1237 h on 19 April.

The top drive was racked back and the drill string was recovered, clearing the rig floor at 1605 h. During the pipe trip, positioning beacon SN 2039 was recovered by 1440 h. The upper guide horn or "piccolo" was then reinstalled, ending operations for Hole U1315A.

Site 642

Hole 642E

Search for Hole 642E Reentry Cone

During the trip out of the hole, the drillship moved back to the original Site 642 prospectus coordinates. From there, a search began for the Hole 642E reentry cone. A 100 × 100 m box pattern search in 15 m swaths was initiated. The operations report for ODP Leg 104 indicated that the reentry cone base was left ~1.0 m below the seafloor, leaving ~1.5–2 m of cone above. Other entries in the report indicated that the last few reentries were difficult and the crew questioned whether future reentries would be possible because they felt that the cone may have been buried in drilled cuttings. It should be noted, however, that all reentries at that time were made using sonar and were not aided by any subsea television capability. The search for the reentry cone began at 2045 h on 19 April and extended through the night without success. The following morning, the ship returned to a target that was not close to where the reentry cone should have been; however, an obvious man-made object was visible on the seafloor and was detected on sonar as well. The object appeared to be an old-style reentry cone reflector. Four of these reflectors were mounted on the older-style reentry cones in the past. Convinced that the cone was buried, we spent several hours attempting to define where a cone might be relative to the single reflector that was visible. Ultimately a stab into the seabed was made with the drill string; however, this was to no avail as the driller noted drill string resistance after lowering the drill string only 9 m into the seabed. Upon reflection, we decided that the object was not the object of our search; the sonar should have identified the remaining cone and reflectors even if submerged. Considering this, coupled with the fact that we were not even close to the area that the cone should have been, we decided to continue on with the search. In so doing, we revisited all that we knew about the location of the target cone and re-

alized that we had started our search pattern at a longitude of 2°55.7′ E, failing to recognize that Hole 642E had in fact been spudded at 2°55.8′ E, a full tenth of a minute off. After entering new offsets into the dynamic positioning system, we finally located the reentry cone on sonar and then ultimately with the subsea television system as well. The cone was fully visible and was not submerged or covered in cuttings. The rim and all four reflectors could be clearly identified, and the cone rim appeared to be, as reported, 1.5 to 2.0 m above the seafloor. Using the new undithered Global Positioning System capabilities of the ship, the ultimate coordinates for Hole 642E are 067°13.1850′ N latitude by 002°55.7789′ E longitude. The cone was actually located 548 m south of Holes 642A and 642B on a bearing of 173°. According to the documentation, the cone should have been located 450 m to the southeast (a bearing of 135°). The drill string was spaced out, and Hole 642E was reentered at 1305 h on 20 April, a total of 16.5 h after the search was initiated.

Wireline Logging

The primary goal of our return to Hole 642E was to obtain a high-resolution continuous temperature log of the hole that had been left undisturbed for nearly 20 y. This hole was drilled to a total depth of 1229.4 mbsf during Leg 104. It was left cased (with $11^3/_4$ inch 54 lb/ft casing) 62.5 m into basement, placing the casing shoe at 371.5 mbsf. To minimize disturbance in the hole, the end of the pipe was placed at only 15.3 mbsf. The LDEO TAP tool was deployed with the standard triple combo (Dual Induction Tool model E [DITE]/Hostile Environment Litho-Density Sonde [HLDS]/Accelerator Porosity Sonde [APS]/Hostile Environment Gamma Ray Sonde [HNGS]) tool string at 1710 h. A good temperature log was obtained on the first run downhole; however, ledges and/or chunks of basalt falling in from above the tools proved to be problematic. After the tools were “mouse trapped” between two such zones for nearly an hour, they were recovered, having only reached a depth of ~1888 mbrf (~599 mbsf) or ~228 m into the open hole below the casing shoe. The first tool suite was recovered at 2225 h on 20 April.

After rigging down the first tool suite, the second suite of tools consisting of the FMS-sonic tool string were made up and deployed. These tools were run in at 0135 h on 21 April and were recovered at 0700 h after reaching a depth of ~1878 mbrf (~589 mbsf) or ~218 m into the open hole.

The FMS-sonic tool string was rigged down, and a final run was made only to 1200 mbsf to test the MGT pressure case. This tool leaked during a logging run earlier in the expedition; however, nothing unusual was found to explain the leak. After clean-

ing the pressure case thoroughly, new O-rings were installed and the body was deployed without electronics to test its pressure integrity. The tools were run in at 0750 h and recovered by 0900 h. The limited test (relatively shallow depth) was successful, and the MGT was recovered without any signs of leakage.

All wireline tools and the Schlumberger logging sheaves were rigged down by 1000 h, and preparations began for drill string recovery. The bit cleared the seafloor/reentry cone at 1005 h, and by 1310 h, all drill pipe had been recovered and all drill collars were laid out to the main deck tubular rack. During the pipe trip, positioning beacon SN 2199 was recovered on deck at 1100 h. The rig floor was secured, all thrusters and hydrophones were raised, and the drillship was under way for Dublin, Ireland, by 1315 h on 21 April 2005.

REFERENCES

Alley, R.B., Clark, P.U., Keigwin, L.D., and Webb, R.S., 1999. Making sense of millennial-scale climate change. *In* Clark, P.U., Webb, R.S., and Keigwin, L.D. (Eds.), *Mechanisms of Global Climate Change at Millennial Time Scales*. Geophys. Monogr., 112:385–394.

Antonov, J.I., 1993. Linear trends of temperature at intermediate and deep layers of the North Atlantic and North Pacific Oceans: 1957–1981. *J. Climate,* 6:1928–1942. **doi:10.1175/1520-0442(1993)006<1928:LTOTAI>2.0.CO;2**

Baldauf, J.G., Thomas, E., Clement, B., Takayama, T., Weaver, P.P.E., Backman, J., Jenkins, G., Mudie, P.J., and Westberg-Smith, M.J., 1987. Magnetostratigraphic and biostratigraphic synthesis, Deep Sea Drilling Project Leg 94. *In* Ruddiman, W.F., Kidd, R.B., Thomas, E., et al., *Init. Repts. DSDP,* 94 (Pt. 2): Washington (U.S. Govt. Printing Office), 1159–1205.

Baumgartner, S., Beer, J., Masarik, J., Wagner, G., Meynadier, L., and Synal, H.-A., 1998. Geomagnetic modulation of the ^{36}Cl flux in the GRIP ice core. *Science,* 279:1330–1332. **doi:10.1126/science.279.5355.1330**

Bond, G., Heinrich, H., Broecker, W., Labeyrie, L.D., McManus, J., Andrews, J., Huon, S., Jantschik, R., Clasen, S., Simet, C., Tedesco, K., Klas, M., Bonani, G., and Ivy, S., 1992. Evidence for massive discharges of icebergs into the North Atlantic Ocean during the last glacial period. *Nature (London, U. K.),* 360:245–249. **doi:10.1038/360245a0**

Bond, G., and Lotti, R., 1995. Iceberg discharges into the North Atlantic on millennial time scales during the last glaciation. *Science,* 26:1005–1010.

Bond, G., Kromer, B., Beer, J., Muscheler, R., Evans, M.N., Showers, W., Hoffmann, S., Lotti-Bond, R., Hajdas, I., and Bonani, G., 2001. Persistent solar influence on North Atlantic climate during the Holocene. *Science,* 294:2130–2136. **doi:10.1126/science.1065680**

Bond, G.C., Broecker, W., Johnsen, S., McManus, J., Labeyrie, L., Jouzel, J., and Bonani, G., 1993. Correlations between climate records from North Atlantic sediments and Greenland ice. *Nature (London, U. K.),* 365:143–147. **doi:10.1038/365143a0**

Bond, G.C., Showers, W., Elliot, M., Evans, M., Lotti, R., Hajdas, I., Bonani, G., and Johnson, S., 1999a. The North Atlantic's 1–2 kyr climate rhythm: relation to Heinrich events, Dansgaard/Oeschger cycles and the Little Ice Age. *In* Clark, P.U., Webb, R.S., and Keigwin, L.D. (Eds.), *Mechanisms of Global Climate Change at Millennial Time Scales*. Geophys. Monogr., 112:35–58.

Bond, G., Showers, W., and Lynch-Stieglitz, J., 1999b. Are major shifts in thermohaline circulation revealed in North Atlantic and South Atlantic antiphased patterns? *Eos, Trans. Am. Geophys. Union,* 80:S169.

Broecker, W.S., 1987. Unpleasant surprises in the greenhouse? *Nature (London, U. K.),* 328:123–126. **doi:10.1038/328123a0**

Calvo, E., Villanueva, J., Grimalt, J.O., Boelaert, A., and Labeyrie, L., 2001. New insights into the glacial latitudinal temperature gradients in the North Atlantic. Results from $U^{k'}_{37}$ sea surface temperatures and terrigenous inputs. *Earth Planet. Sci. Lett.,* 188:509–519. **doi:10.1016/S0012-821X(01)00316-8**

Campbell, I.D., Campbell, C., Apps, M.J., Rutter, N.W., and Bush, A.B.G., 1998. Late Holocene ~1500 yr climatic periodicities and their implications. *Geology,* 26:471–473. **doi:10.1130/0091-7613(1998)026<0471:LHYCPA>2.3.CO;2**

Cande, S.C., and Kent, D.V., 1995a. A new geomagnetic polarity time scale for the Late Cretaceous and Cenozoic. *J. Geophys. Res.,* 97:13917–13951.

Cande, S.C., and Kent, D.V., 1995b. Revised calibration of the geomagnetic polarity timescale for the Late Cretaceous and Cenozoic. *J. Geophys. Res.,* 100:6093–6095. **doi:10.1029/94JB03098**

Carlut J., and Courtillot, V., 1998. How complex is the time-averaged geomagnetic field over the past 5 myr? *Geophys. J. Int.,* 134:527–544. **doi:10.1046/j.1365-246x.1998.00577.x**

Channell, J.E.T., Hodell, D.A., McManus, J., and Lehman, B., 1998. Orbital modulation of the Earth's magnetic field intensity. *Nature (London, U. K.),* 394:464–468. **doi:10.1038/28833**

Channell, J.E.T., and Lehman, B., 1997. The last two geomagnetic polarity reversals recorded in high-deposition-rate sediment drifts. *Nature (London, U. K.),* 389:712–715. **doi:10.1038/39570**

Channell, J.E.T., Mazaud, A., Sullivan, P., Turner, S., and Raymo, M.E., 2002. Geomagnetic excursions and paleointensities in the Matuyama Chron at ODP Sites 983 and 984 (Iceland Basin). *J. Geophys. Res.,* 107. **doi:10.1029/2001JB000491**

Channell, J.E.T., Sato, T., Kanamatsu, T., Stein, R., Malone, M.J., and the Expedition 303/306 Project Team, 2004. North Atlantic climate. *IODP Sci. Prosp.,* 303/306. **doi:10.2204/IODP.SP.303306.2004**

Channell, J.E.T., Sato, T., Malone, M.J., and Expedition Scientists, in press. *Proc. IODP,* 303: College Station TX (Integrated Ocean Drilling Program Management International).

Channell, J.E.T., Stoner, J.S., Hodell, D.A., and Charles, C.D., 2000. Geomagnetic paleointensity for the last 100 kyr from the sub-antarctic South Atlantic: a tool for inter-hemispheric correlation. *Earth Planet. Sci. Lett.,* 175:145–160. **doi:10.1016/S0012-821X(99)00285-X**

Chapman, D.S., and Harris, R.N., 1993. Repeat temperature measurements in Borehole GC-1, northwestern Utah: towards isolating a climate-change signal in borehole temperature profiles. *Geophys. Res. Lett.,* 18:1891–1894.

Clark, P.U., Webb, R.S., and Keigwin, L.D., (Eds.), 1999. *Mechanisms of Global Climate Change at Millennial Time Scales*. Geophys. Monogr., Vol. 112.

CLIMAP Project Members, 1976. The surface of the ice-age Earth. *Science,* 191:1131–1137.

Coe, R.S., Hongre, L., and Glatzmaier, G.A., 2000. An examination of simulated geomagnetic reversals from a palaeomagnetic perspective. *Philos. Trans. R. Soc. London, Ser. A,* 358:1141–1170.

Crowley, T.J., 1999. Correlating high-frequency climate variations. *Paleoceanography,* 14:271–272. **doi:10.1029/1999PA900003**

De Graciansky, P.C., Poag, C.W., et al., 1985. *Init. Reps. DSDP,* 80: Washington (U.S. Govt. Printing Office).

deMenocal, P., Ortiz, J., Guilderson, T., and Sarnthein, M., 2000. Coherent high- and low-latitude variability during the Holocene warm period. *Science,* 288:2198–2202. **doi:10.1126/science.288.5474.2198**

Dickson, B., 1997. From the Labrador Sea to global change. *Nature (London, U. K.),* 386:649–650. **doi:10.1038/386649a0**

Eldholm, O., Thiede, J., Taylor, E., et al., 1987. *Proc. ODP, Init. Repts.,* 104: College Station, TX (Ocean Drilling Program).

Elliot, M., Labeyrie, L., Dokken, T., and Manthe, S., 2001. Coherent patterns of ice-rafted debris deposits in the Nordic regions during the last glacial (10–60 ka). *Earth Planet. Sci. Lett.,* 194:151–163. **doi:10.1016/S0012-821X(01)00561-1**

Flower, B.P., Oppo, D.W., McManus, J.F., Venz, K.A., Hodell, D.A., and Cullen, J., 2000. North Atlantic Intermediate to Deep Water circulation and chemical stratification during the past 1 Myr. *Paleoceanography,* 15:388–403. **doi:10.1029/1999PA000430**

Frank, M., Schwarz, B., Baumann, S., Kubik, P.W., Suter, M., and Mangini, A., 1997. A 200 kyr record of cosmogenic radionuclide production rate and geomagnetic field intensity from ^{10}Be in globally stacked deep-sea sediments. *Earth Planet. Sci. Lett.,* 149:121–129. **doi:10.1016/S0012-821X(97)00070-8**

Fronval, T., Jansen, E., Bloemendal, J., and Johnson, S., 1997. Oceanic evidence for coherent fluctuations in Fennoscandian and Laurentide ice sheets on millennial time scales. *Nature (London, U. K.),* 374:443–446. **doi:10.1038/374443a0**

Gammelsrød, T., Østerhus, S., and Godøy, Ø., 1992. Decadal variations of ocean climate in the Norwegian Sea at Ocean Station "Mike" (65°N 2°E). *ICES J. Mar. Sci.,* 195:68–75.

Glatzmaier, G.A., and Roberts, P.H., 1995. A 3-dimensional self-consistent computer-simulation of a geomagnetic-field reversal. *Nature (London, U. K.),* 377:203–209. **doi:10.1038/377203a0**

Gubbins, D., 1999. The distinction between geomagnetic excursions and reversals. *Geophys. J. Int.,* 137:F1–F3. **doi:10.1046/j.1365-246x.1999.00810.x**

Guyodo, Y., Gaillot, P., and Channell, J.E.T., 2000. Wavelet analysis of relative geomagnetic paleointensity at ODP Site 983. *Earth Planet. Sci. Lett.,* 184:109–123. **doi:10.1016/S0012-821X(00)00313-7**

Guyodo, Y., and Valet, J.-P., 1996. Relative variations in geomagnetic intensity from sedimentary records: the past 200,000 years. *Earth. Planet. Sci. Lett.,* 143:23–36. **doi:10.1016/0012-821X(96)00121-5**

Hongre, L., Hulot, G., and Khokhlov, A., 1998. An analysis of the geomagnetic field over the past 2000 years. *Phys. Earth Planet. Inter.,* 106:311–335.

Hulot, G., and Le Mouël, J.-L., 1994. A statistical approach to the Earth's main magnetic field. *Phys. Earth Planet. Inter.,* 82:167–183.

Johnson, C.L., and Constable, C.G., 1997. The time-averaged geomagnetic field: global and regional biases for 0–5 Ma. *Geophys. J. Int.,* 131:643–666.

Kanamatsu, T., Stein, R., and Alvarez Zarikian, C.A., 2005. North Atlantic climate II addendum. *IODP Sci. Prosp.,* 306 Add. **doi:10.2204/IODP.SP.303306add.2005**

Keigwin, L.D., Rio, D., Acton, G.D., et al., 1998. *Proc. ODP, Init. Repts.,* 172: College Station, TX (Ocean Drilling Program).

Kelly, P., and Gubbins, D., 1997. The geomagnetic field over the past 5 million years. *Geophys. J. Int.,* 128:315–330.

Kissel, C., Laj, C., Labeyrie, L., Dokken, T., Voelker, A., and Blamart, D., 1999. Rapid climatic variations during climatic stage 3: magnetic analysis of North Atlantic sediments. *Earth Planet. Sci. Lett.,* 171:489–502. **doi:10.1016/S0012-821X(99)00162-4**

Kleiven, H.F., Jansen, E., Curry, W.B., Hodell, D.A., and Venz, K., 2003. Atlantic Ocean thermohaline circulation changes on orbital to suborbital timescales during the mid-Pleistocene. *Paleoceanography,* 18. **doi:10.1029/2001PA000629**

Laj, C., Kissel, C., Mazaud, A., Channell, J.E.T., and Beer, J., 2000. North Atlantic paleointensity stack since 75 ka (NAPIS-75) and the duration of the Laschamp Event. *Phil. Trans. R. Soc. Lond.,* 358:1009–1025.

Larsen, H.C., Saunders, A.D., Clift, P.D., et al., 1994. *Proc. ODP, Init. Reps.* 152, College Station, TX (Ocean Drilling Program).

Lisiecki, L.E. and Raymo, M.E., 2005. A Pliocene-Pleistocene stack of 57 globally distributed benthic $\delta^{18}O$ records. *Paleoceanography,* 20. **doi:10.1029/2004PA001071**

Lund, S.P., Acton, G., Clement, B., Hastedt, M., Okada, M., and Williams, T., 1998. Geomagnetic field excursions occurred often during the last million years. *Eos, Trans. Am. Geophys. Union,* 79:178–179.

Lund, S.P., Acton, G.D., Clement, B., Okada, M., and Williams, T., 2001. Paleomagnetic records of Stage 3 excursions, Leg 172. *In* Keigwin, L.D., Rio, D., Acton, G.D., and Arnold, E. (Eds.), *Proc. ODP, Sci. Results,* 172, 1–20 [Online]. Available from World Wide Web: <**http://www-odp.tamu.edu/publications/172_SR/VOLUME/CHAPTERS/SR172_11.PDF**>.

Lund, S.P., Williams, T., Acton, G., Clement, B., and Okada, M., 2001b. Brunhes Chron magnetic-field excursions recovered from Leg 172 sediments. *In* Keigwin, L.D., Rio, D., Acton, G.D., and Arnold, E. (Eds.), *Proc. ODP, Sci. Results,* 172, 1–18 [Online]. Available from World Wide Web: <**http://www-odp.tamu.edu/publications/172_SR/VOLUME/CHAPTERS/SR172_10.PDF**>.

Mazaud, A., Laj, C., and Bender, M., 1994. A geomagnetic chronology for Antarctic ice accumulation. *Geophys. Res. Lett.,* 21:337–340. **doi:10.1029/93GL02789**

McManus, J., Bond, G., Broecker, W., Johnsen, S., Laybeyrie, L., and Higgins, S., 1994. High resolution climate records from the North Atlantic during the last interglacial. *Nature (London, U. K.),* 371:326–329. **doi:10.1038/371326a0**

McManus, J.F., Oppo, D.W., and Cullen, J.L., 1999. A 0.5 million year record of millennial-scale climate variability in the North Atlantic. *Science,* 283:971–975. **doi:10.1126/science.283.5404.971**

Meynadier, L., Valet, J.-P., Weeks, R.J., Shackleton, N.J., and Hagee, V.L., 1992. Relative geomagnetic intensity of the field during the last 140 ka. *Earth Planet. Sci. Lett.,* 114:39–57. **doi:10.1016/0012-821X(92)90150-T**

Mudelsee, M., and Schultz, M., 1997. The mid-Pleistocene climate transition: onset of 100 ka cycle lags ice volume built-up by 280 ka. *Earth Planet. Sci. Lett.,* 151:117–123. **doi:10.1016/S0012-821X(97)00114-3**

Oppo, D.W., McManus, J.F., and Cullen, J.L., 1998. Abrupt climate events 500,000 to 340,000 years ago: evidence from subpolar North Atlantic sediments. *Science,* 279:1335–1338. **doi:10.1126/science.279.5355.1335**

Pflaumann, U., Sarnthein, M., Chapman, M., de Abreu, L., Funnell, B., Huels, M., Kiefer, T., Maslin, M., Schulz, H., Swallow, J., van Kreveld, S., Vautravers, M., Vogelsang, E. and Weinelt, M., 2003. *Paleoceanography,* 18(3). **doi:10.1029/2002PA000774**

Poli, M.S., Thunell, R.C., and Rio, D., 2000. Millennial-scale changes in North Atlantic Deep Water circulation during marine isotope Stages 11 and 12: linkage to Antarctic climate. *Geology,* 28:807–810. **doi:10.1130/0091-7613(2000)028<0807:MSCINA>2.3.CO;2**

Raisbeck G.M., Yiou, F., Bourles, D., Lorius, C., Jouzel, J., and Barkov, N.I., 1987. Evidence for two intervals of enhanced ^{10}Be deposition in Antarctic ice during the last glacial period. *Nature (London, U. K.),* 326:273–277. **doi:10.1038/326273a0**

Raymo, M.E., 1999. Appendix. New insights into Earth's history: an introduction to Leg 162 postcruise research published in journals. *In* Raymo, M.E., Jansen, E., Blum, P., and Herbert, T.D. (Eds.), *Proc. ODP, Sci. Results,* 162: College Station, TX (Ocean Drilling Program), 273–275.

Raymo, M.E., Ganley, K., Carter, S., Oppo, D.W., and McManus, J., 1998. Millennial-scale climate instability during the early Pleistocene epoch. *Nature (London, U. K.),* 392:699–702. **doi:10.1038/33658**

Raymo, M.E., Oppo, D.W., Flower, B.P., Hodell, D.A., McManus, J.F., Venz, K.A., Kleiven, K.F., and McIntyre, K., 2004. Stability of North Atlantic water masses in face of pronounced climate variability during the Pleistocene. *Paleoceanography,* 19. **doi:10.1029/2003PA000921**

Raymo, M.E., Ruddiman, W.F., Backman, J., Clement, B.M., and Martinson, D.G., 1989. Late Pliocene variation in Northern Hemisphere ice sheets and North Atlantic Deep Water circulation. *Paleoceanography,* 4:413–446.

Roemmich, D., and Wunsch, C., 1984. Apparent changes in the climatic state of the deep North Atlantic Ocean. *Nature (London, U. K.),* 307:447–450. **doi:10.1038/307447a0**

Ruddiman, W.F., Kidd, R.B., Thomas, E., et al., 1987. *Init. Repts. DSDP,* 94 (Pts. 1 and 2): Washington (U.S. Govt. Printing Office).

Ruddiman, W.F., Raymo, M., and McIntyre, A., 1986. Matuyama 41,000-year cycles: North Atlantic Ocean and Northern Hemisphere ice sheets. *Earth Planet. Sci. Lett.,* 80:117–129. **doi:10.1016/0012-821X(86)90024-5**

Ruddiman, W.F., Raymo, M.E., Martinson, D.G., Clement, B.M., and Backman, J., 1989. Pleistocene evolution: Northern Hemisphere ice sheets and North Atlantic Ocean. *Paleoceanography,* 4:353–412.

Sarnthein, M., Stattegger, K., Dreger, D., Erlenkeuser, H., Grootes, P., Haupt, B.J., Jung, S., Kiefer, T., Kuhnt, W., Pflaumann, U., Schäfer-Neth, C., Schulz, H., Schulz, M., Seidov, D., Simstich, J., van Kreveld, S., Vogelsang, E., Völker, A., and Weinelt, M., 2000. Fundamental modes and abrupt changes in North Atlantic circulation and climate over the last 60 ky—concepts, reconstruction and numerical modeling. *In* Schäfer, P., Ritzrau, W., Schlüter, M., and Thiede, J. (Eds.), *The Northern Atlantic: A Changing Environment:* Berlin (Springer-Verlag), 365–410.

Schmieder, F., von Dobeneck, T., and Bleil, U., 2000. The mid-Pleistocene climate transition as documented in the deep South Atlantic Ocean: initiation, interim state and terminal event. *Earth Planet. Sci. Lett.,* 179:539–549. **doi:10.1016/S0012-821X(00)00143-6**

Shipboard Scientific Party, 2005. North Atlantic climate: ice sheet-ocean atmosphere interactions on millennial timescales during the late Neogene–Quaternary using a paleointensity-assisted chronology for the North Atlantic. *IODP Prel. Rept.,* 303. **doi:10.2204/IODP.PR.303.2005**

Sirocko, F., Garbe-Schönberg, D., McIntyre, A., and Molfino, B., 1996. Teleconnections between the subtropical monsoons and high-latitude climates during the last deglaciation. *Science,* 272:526–529.

Stoner, J.S., Channell, J.E.T., and Hillaire-Marcel, C., 1998. A 200 ka geomagnetic chronostratigraphy for the Labrador Sea: indirect correlation of the sediment record to SPECMAP. *Earth Planet. Sci. Lett.,* 159:165–181. **doi:10.1016/S0012-821X(98)00069-7**

Stoner, J.S., Channell, J.E.T., Hillaire-Marcel, C., and Kissel, C., 2000. Geomagnetic paleointensity and environmental record from Labrador Sea Core MD95-2024: global marine sediment and ice core chronostratigraphy for the last 110 kyr. *Earth Planet. Sci. Lett.,* 183:161–177. **doi:10.1016/S0012-821X(00)00272-7**

Stoner, J.S., Laj, C., Channell, J.E.T., and Kissel, C., 2002. South Atlantic (SAPIS) and North Atlantic (NAPIS) geomagnetic paleointensity stacks (0–80 ka): implications for interhemispheric correlation. *Quat. Sci. Rev.,* 21:1142–1151.

van Kreveld, S., Sarnthein, M., Erlenkeuser, H., Grootes, P., Jung, S., Nadeau, M.J., Pflaumann, U., and Voelker, A., 2000. Potential links between surging ice sheets, circulation changes and the Dansgaard/Oeschger cycles in the Irminger Sea, 60–18 kyr. *Paleoceanography,* 15:425–442. **doi:10.1029/1999PA000464**

Voelker, A.H.L., Sarnthein, M., Grootes, P.M., Erlenkeuser, H., Laj, C., Mazaud, A., Nadeau, M.-J., and Schleicher, M., 1998. Correlation of marine ^{14}C ages from the Nordic Seas with the GISP2 isotope record: implications for ^{14}C calibration beyond 25 ka BP. *Radiocarbon,* 40:517–534.

Woods, R.A., Keen, A.B., Mitchell, J.R.B., and Gregory, J.M., 1999. Changing spatial structure of thermohaline circulation in response to atmospheric CO_2 forcing in a climate model. N*ature (London, U. K.),* 399:572–575. **doi:10.1038/21170**

Wunsch, C., 1992. Decade-to-century changes in the ocean circulation. *Oceanography,* 5:99–106.

Yamazaki, T., 1999. Relative paleointensity of the geomagnetic field during Brunhes Chron recorded in North Pacific deep-sea sediment cores: orbital influence? *Earth Planet. Sci. Lett.,* 169:23–35. **doi:10.1016/S0012-821X(99)00064-3**

Table T1. Events and corresponding composite depth.

Biostratigraphic event	Age (Ma)	Event depth (mcd)		
		Site U1312	Site U1313	Site U1314
LO *Helicosphaera inversa*	0.16		8.375	
FO *Emiliania huxleyi*	0.25	13.47	19.105	25.565
LO *Rhizosolenia curvirostris*	0.30			22.845
LO *Pseudoemiliania lacunosa*	0.41	13.47	21.205	32.285
LO *Fragilariopsis reinholdii*	0.50	20.565	34.505	39.35
FO *Helicosphaera inversa*	0.51		22.09	61.4
LO *Fragilariopsis fossilis*	0.70			57.565
LO *Neodenticula seminae*	0.84			65.27
LO *Reticulofenestra asanoi*	0.85		24.815	69.01
FO *Gephyrocapsa parallela*	0.95	18.41	47.035	74.235
LO *Stilostomella lepidula*	1.00		47.035	87.37
FO *Reticulofenestra asanoi*	1.16		54.31	94.435
LO large *Gephyrocapsa* spp.	1.21	22.775	51.815	94.435
FO *Neodenticula seminae*	1.25			104.355
LO *Helicosphaera sellii*	1.27	25.31	61.955	97.53
FO large *Gephyrocapsa* spp.	1.45	31.96	79.4	126.535
FO *Rhizosolenia curvirostris*	1.52			154.295
FO *Gephyrocapsa oceanica*	1.65			150.73
FO *Gephyrocapsa caribbeanica*	1.73	37.95	87.41	155.855
FaO *Neogloboquadrina pachyderma* (sinistral)	1.78		83	157.71
LO *Discoaster brouweri*	1.97	28	91.635	174.675
FO *Globorotalia truncatulinoides*	2.08	39.15	99.965	
FO *Globorotalia inflata*	2.09	39.15	108.94	184.815
LO *Discoaster pentaradiatus*	2.38	28	110.695	232.9
LO *Thalassiosira convexa*	2.40	52.28		241.18
LO *Globorotalia miocenica*	2.40		107.11	
LO *Neogloboquadrina atlantica* (sinistral)	2.41			221.065
LO *Globorotalia puncticulata*	2.41	55	103.66	222.94
LO *Discoaster surculus*	2.54	40.7	121.04	253.365
FO *Cycladophora davisiana*	2.59	56.525		
LO *Spongaster tetras?*	2.60			272.955
LO *Discoaster tamalis*	2.74	37.4	114.35	272.955
Disappearance *Globorotalia hirsuta*	3.18	52.28	151.875	
LO *Sphaeroidinellopsis seminulina*	3.19	56.525	147.445	
Reappearance *Globorotalia puncticulata*	3.31	103	153.69	
Disappearance *Globorotalia puncticulata*	3.57	112.48	164.09	
LO *Globorotalia margaritae*	3.81		183.77	
LO *Reticulofenestra pseudoumbilicus*	3.85	117.8	172.87	
LcO *Globorotalia margaritae*	3.98	124.49	185.67	
FO *Globorotalia puncticulata*	4.52	144.155	214.85	
FO *Globorotalia crassaformis*	4.52		214.85	
LO *Globigerina nepenthes*	4.89		224.875	
FO *Ceratolithus cristatus* (*rugosus*)	5.089		242.15	
LO *Discoaster quinqueramus*	5.537	173.05	251.94	
LO *Amaurolithus amplificus*	5.999	184.265	320.285	
FaO *Globorotalia margaritae*	6.00	181.5		
Coiling change *Neogloboquadrina pachyderma* s/d	6.30	173		
FO *Amaurolithus amplificus*	6.84	192.2		
FcO gr *Globorotalia miotumida*	7.24	191.5		
FO *Amaurolithus primus*	7.39	191.65		
LO *Globorotalia menardii* 4	7.51	191.65		
Coiling change *Neogloboquadrina pachyderma* d/s	7.80	188.63		
FO *Discoaster berggrenii*	8.28	200.955		
FO *Discoaster loeblichii*	8.43	214.63		
LO *Globorotalia lenguaensis*	8.99	210.915		
FO *Minylitha convallis*	9.43	224.07		
LO *Discoaster hamatus*	9.64	206.73		
FO *Discoaster hamatus*	10.48	252.615		
FcO *Neogloboquadrina pachyderma* morphotype *acostaensis*	10.50	252.615		
LO *Coccolithus miopelagicus*	10.95	252.615		

Notes: Events and corresponding mcd used for Figure **F5.** Shaded events not used to calculate sedimentation rates. Dark blue = nannofossils, pink = foraminifers, light blue = diatoms, orange = radiolarians. FO = first occurrence, LO = last occurrence, FcO = first common occurrence, FaO = first abundant occurrence. s/d = sinistral/dextral. gr = group.

Table T2. Expedition 306 site summary.

Hole	Latitude	Longitude	Depth (mbrf)	Cores (*N*)	Cored (m)	Recovered (m)	Recovery (%)	Drilled (m)	Total penetration (m)	Total depth (mbrf)	Time on hole (h)	Time on hole (days)
U1312A	42°50.2040′N	23°05.2506′W	3533.0	25	237.5	248.07	104.5	0.0	237.5	3770.5	47.25	2.0
U1312B	42°50.2150′N	23°5.2652′W	3533.6	25	231.9	236.84	102.1	0.0	231.9	3765.5	59.00	2.5
		Site U1312 totals:		50	469.4	484.91	103.3	0.0	469.4	NA	106.25	4.4
U1313A	41°0.0679′N	32°57.4386′W	3423.3	33	308.6	319.64	103.6	0.0	308.6	3731.9	46.50	1.9
U1313B	41°0.0818′N	32°57.4380′W	3424.6	32	300.4	306.54	102.0	2.0	302.4	3727.0	48.25	2.0
U1313C	41°0.0805′N	32°57.4206′W	3423.8	32	293.4	305.79	104.2	0.0	293.4	3717.2	32.50	1.4
U1313D	41°0.0667′N	32°57.4214′W	3423.0	16	152.0	159.27	104.8	0.0	152.0	3575.0	22.75	0.9
		Site U1313 totals:		113	1054.4	1091.24	103.5	2.0	1056.4	NA	150.00	6.3
U1314A	56°21.8826′N	27°53.3091′W	2810.6	28	258.4	267.34	103.5	0.0	258.4	3069.0	31.50	1.3
U1314B	56°21.8964′N	27°53.3107′W	2811.5	30	279.5	285.36	102.1	0.0	279.5	3091.0	25.00	1.0
U1314C	56°21.8957′N	27°53.2867′W	2810.3	22	207.7	212.93	102.5	0.0	207.7	3018.0	27.75	1.2
		Site U1314 totals:		80	745.6	765.63	102.7	0.0	745.6	NA	84.25	3.5
U1315A	67°12.74.06′N	2°56.2420′E	1283.0	0	0.0	0.00	0.0	179.1	179.1	1462.1	101.50	4.2
		Site U1315 totals:		0	0.0	0.00	0.0	179.1	179.1	1462.1	101.50	4.2
642E	67°13.1850′N	2°55.7789′E	1289.0	0	0.0	0.00	0.0	0.0	0.0	1289.0	44.50	1.9
		Site 642 totals:		0	0.0	0.00	0.0	0.0	0.0	NA	44.50	1.9
		Expedition 306 totals:		243	2269.4	2341.78	103.2	181.1	2450.5	NA	486.50	20.3

Notes: *N* = number. NA = not applicable.

Figure F1. Locations of Expedition 303 and 306 sites.

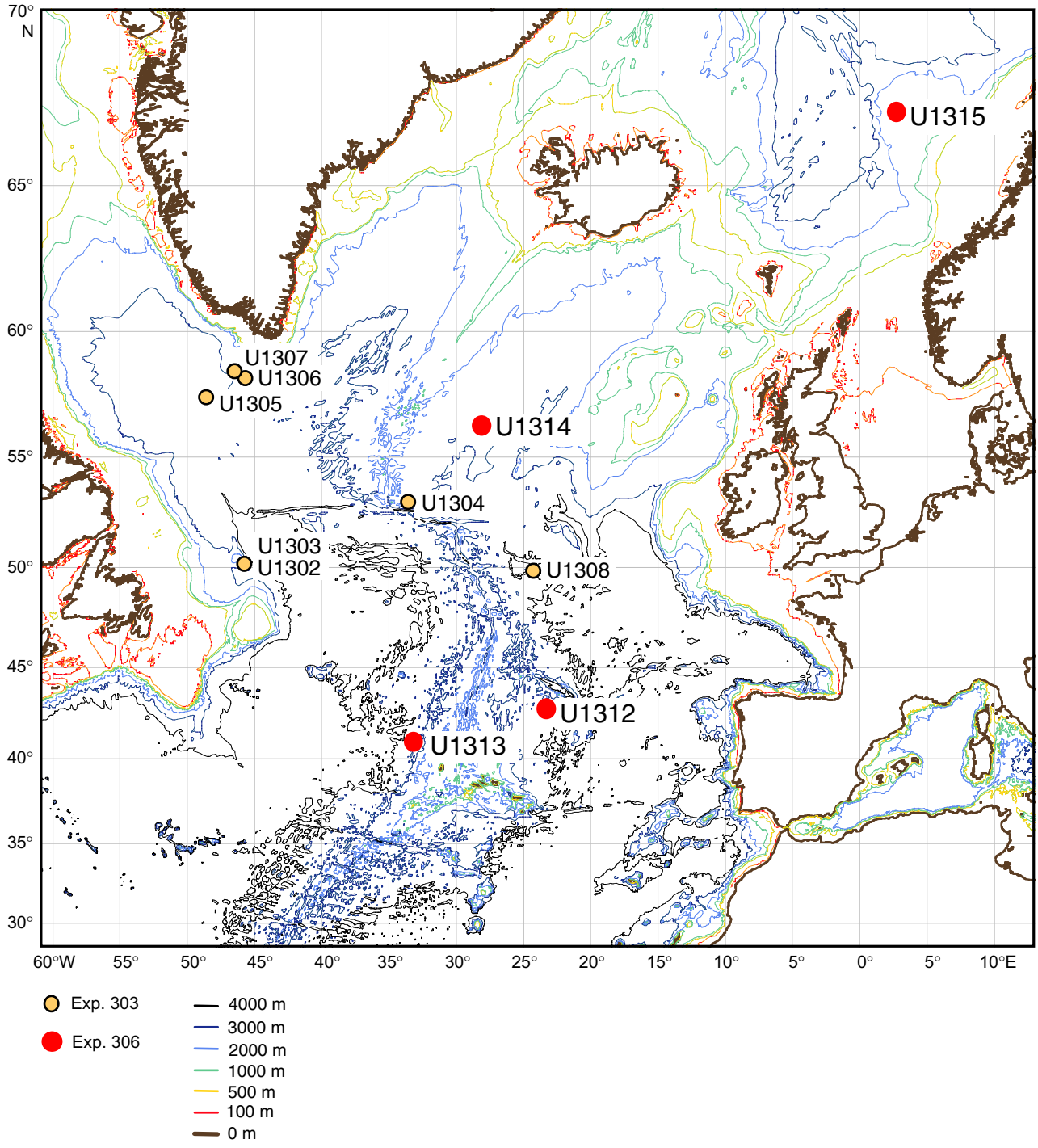

Figure F2. Map showing modern circulation in the North Atlantic, locations of Expedition 303 and 306 sites (blue and red circles, respectively) and Leg 162 sites (green circles) (discussed in the text), and the distribution of rock types that are potential source areas of detrital carbonate. Large blue arrows = pathways of detrital matter supplied during Heinrich events, gray field = Ruddiman's ice-rafted debris (IRD) belt (from Bond and Lotti, 1995).

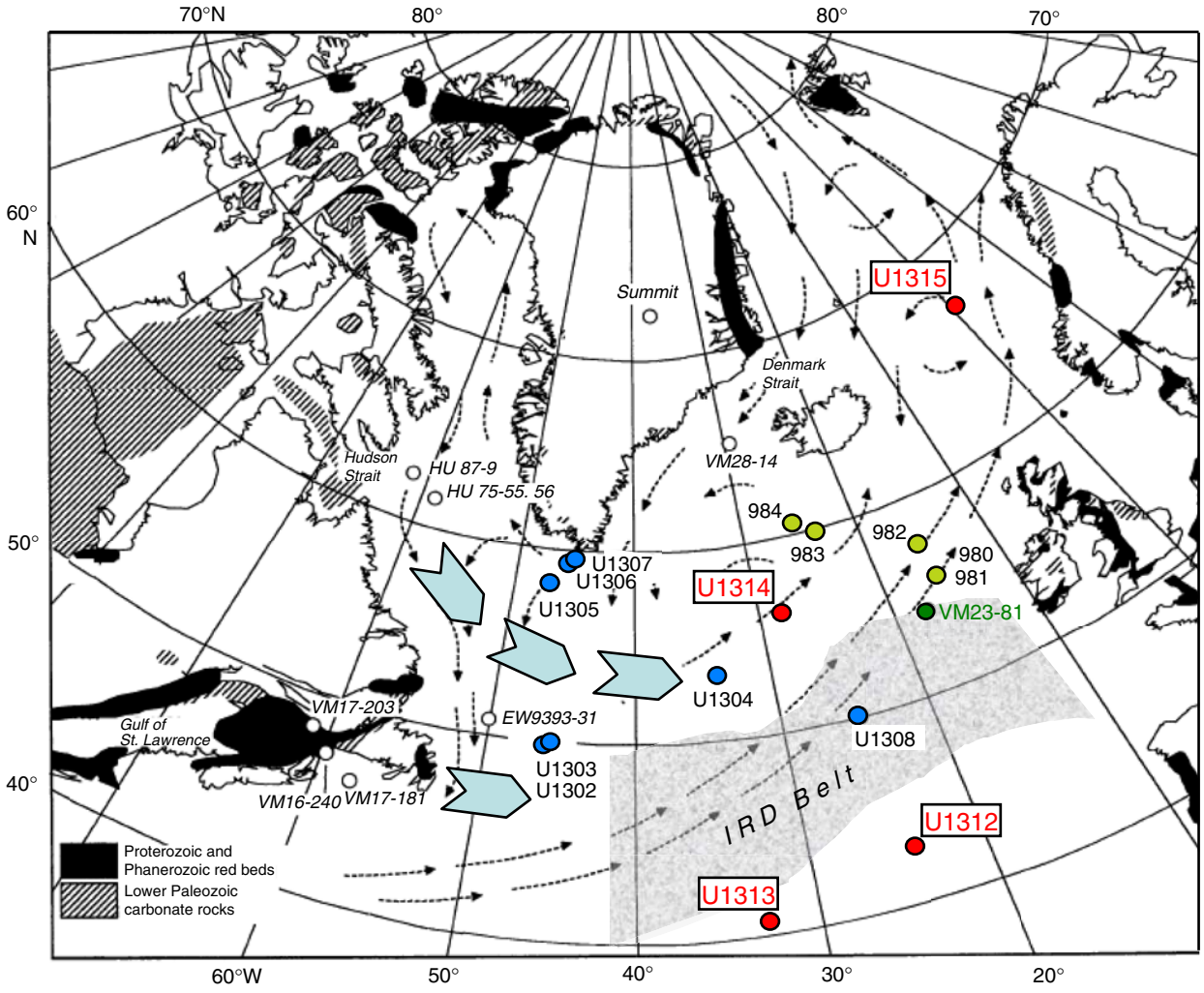

Figure F3. Location map of the Norwegian Sea and Vøring Plateau showing ODP Hole 642E and location of ocean weather ship station (OWS) Mike (modified from Gammelsrød et al., 1992).

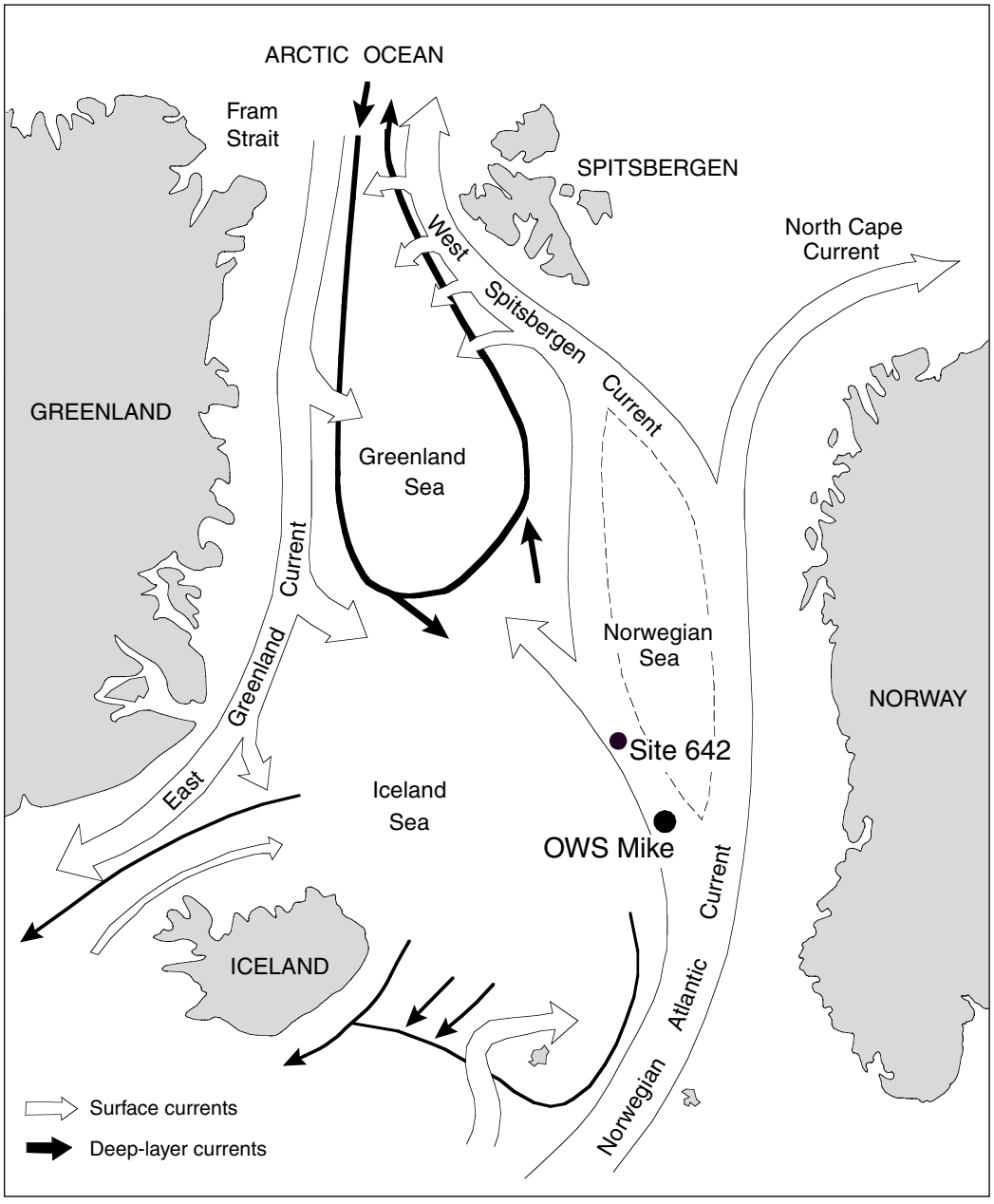

Figure F4. Lithology of Expedition 306 sites.

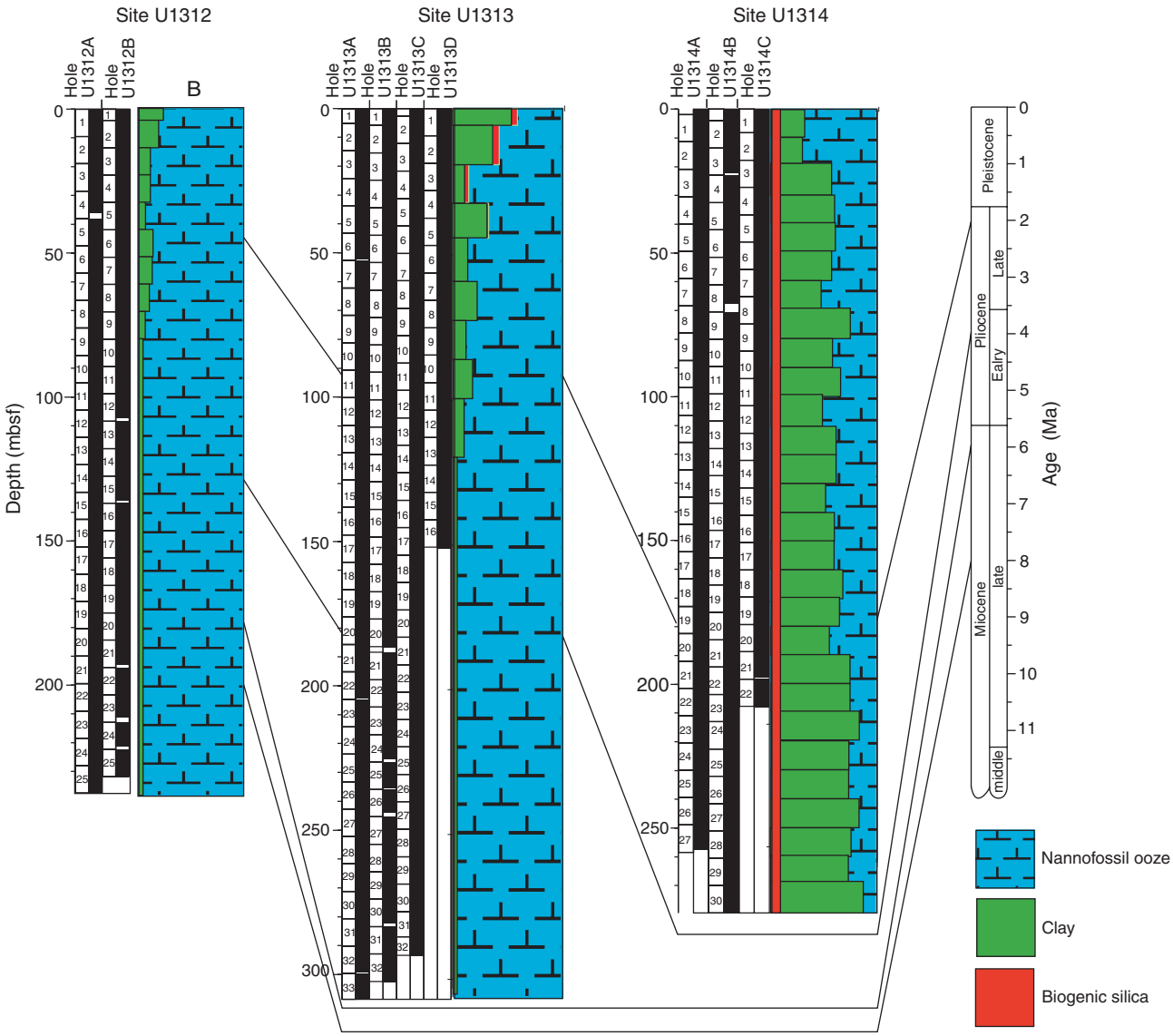

Figure F5. Sedimentation rates at sites drilled during Expedition 306. Open squares = magnetostratigraphy-based ages, solid circles = nannofossil-based ages, solid triangles = foraminifer-based ages, solid squares = diatom-based ages, solid diamonds = radiolarian-based ages. Mean sedimentation rates are calculated for straight-line segments. Unreliable points are faded and not used for calculation of sedimentation rates. These points are events that may be reworked, may not represent true first or last occurrences because of distribution limits within different water masses, or resulted in incongruous depths when plotted on the mcd scale.

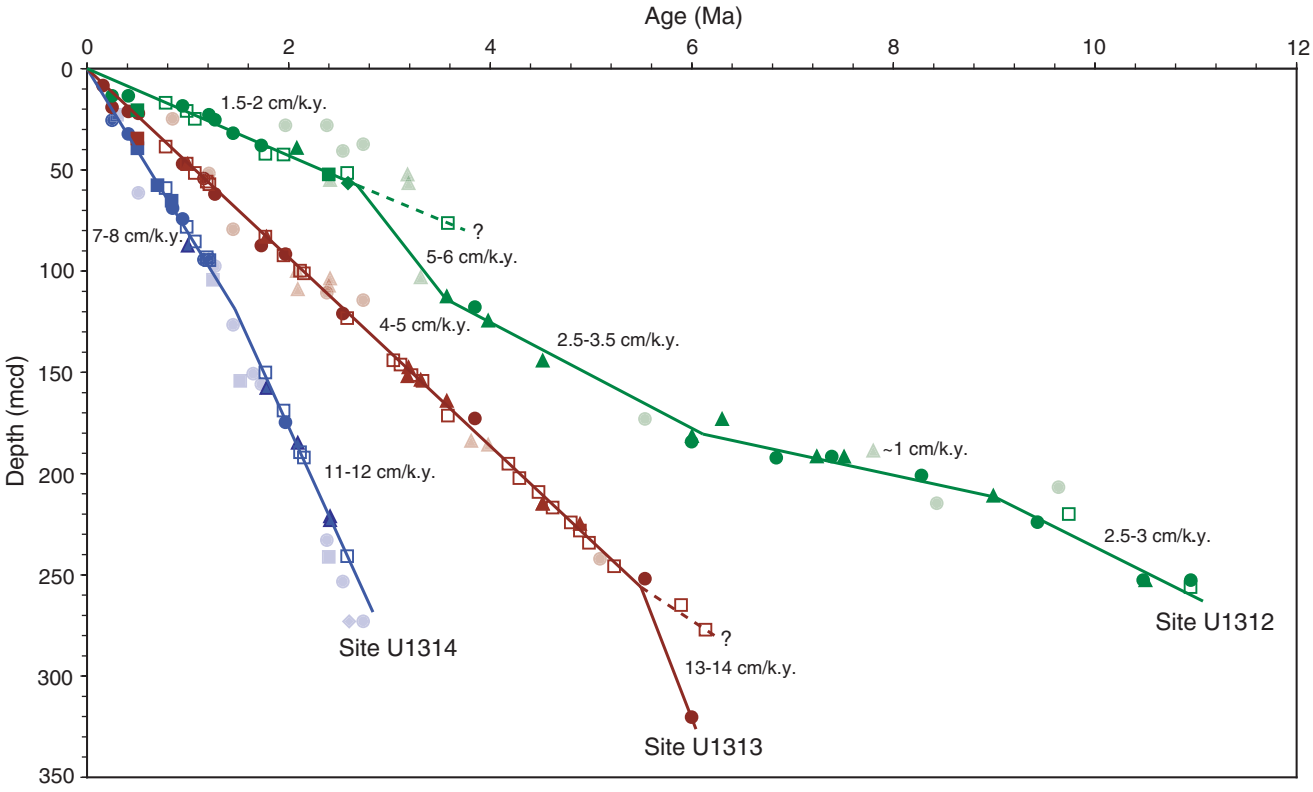

Figure F6. Expedition 306 schematic magnetostratigraphy. The paleomagnetic polarity interpretations (black = normal polarity, white = reversed polarity, gray = undetermined polarity) were obtained on the basis of inclination data acquired after 20 mT AF demagnetization. The reference geomagnetic polarity timescale is displayed on the right side of the figure (Cande and Kent, 1995). Continuous blue lines = main tie points used to establish the age models.

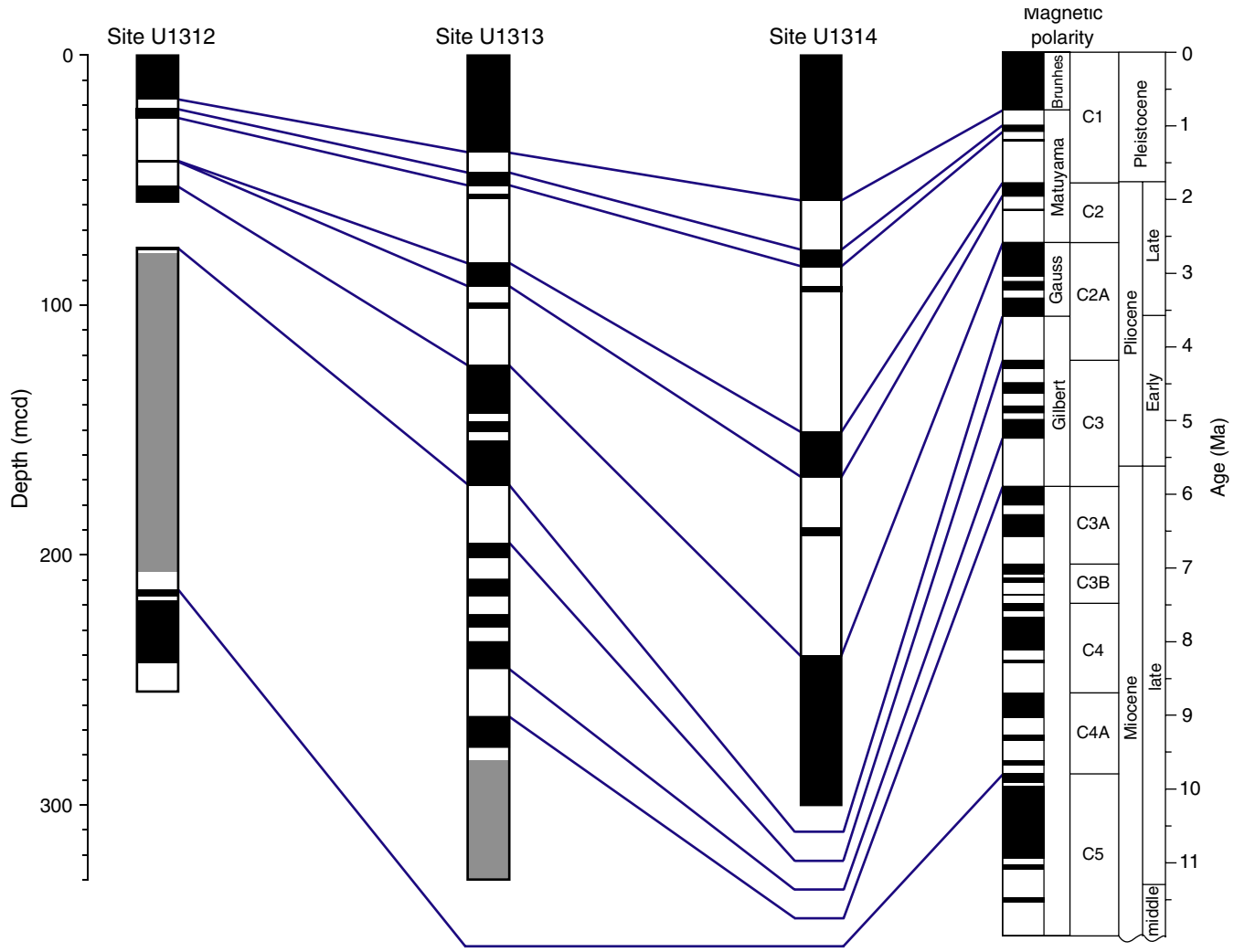

Figure F7. Core recovery, natural gamma ray (NGR) counts, magnetic susceptibility, and gamma ray attenuation (GRA) density measurements from the MST and AMST reflectance (L*) values in the sedimentary record of Site U1312. Gray = cored, black = recovered.

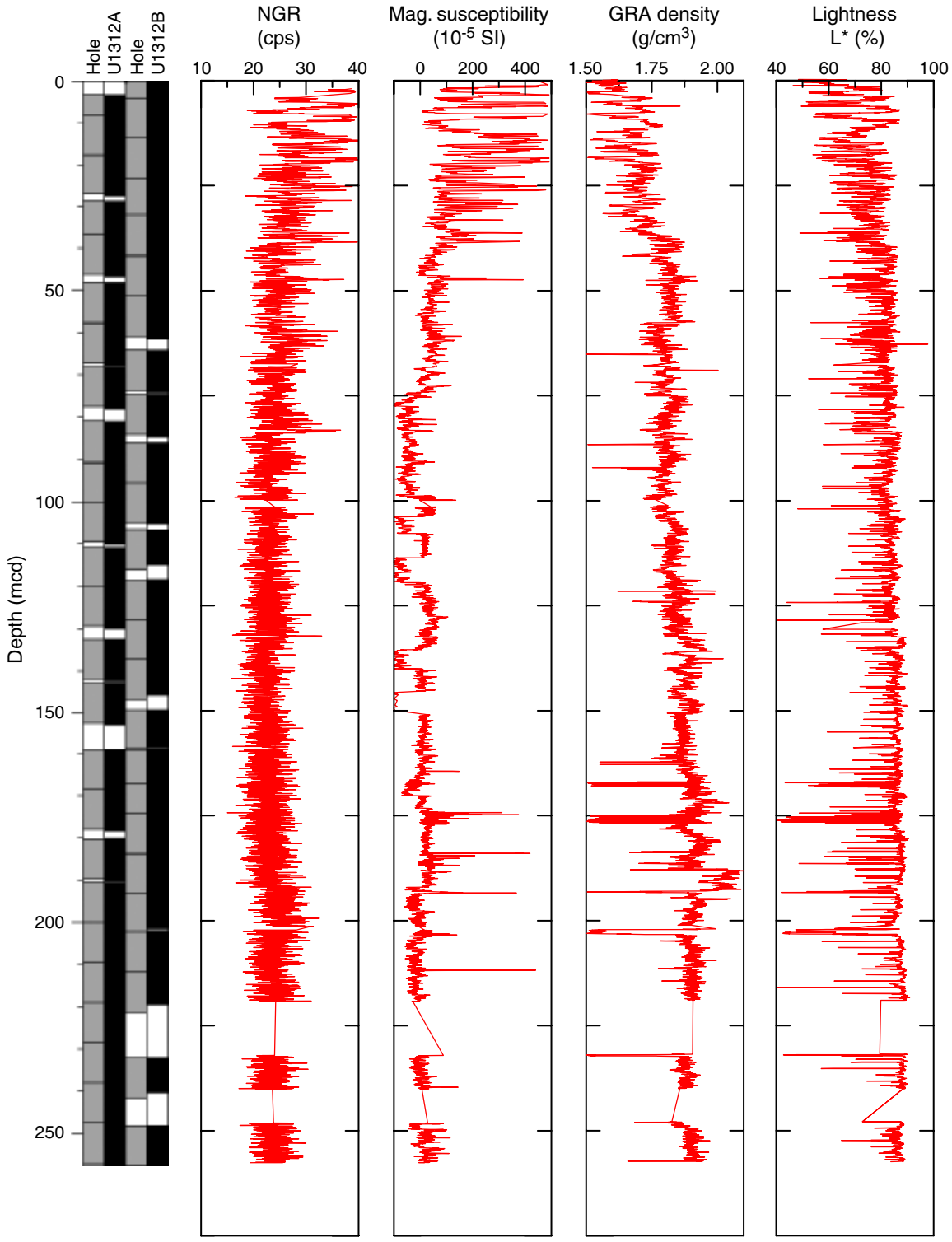

Figure F8. Core recovery, natural gamma ray (NGR) counts, magnetic susceptibility, and gamma ray attenuation (GRA) density measurements from the MST and AMST reflectance (L*) values in the sedimentary record of Site U1313. Gray = cored, black = recovered.

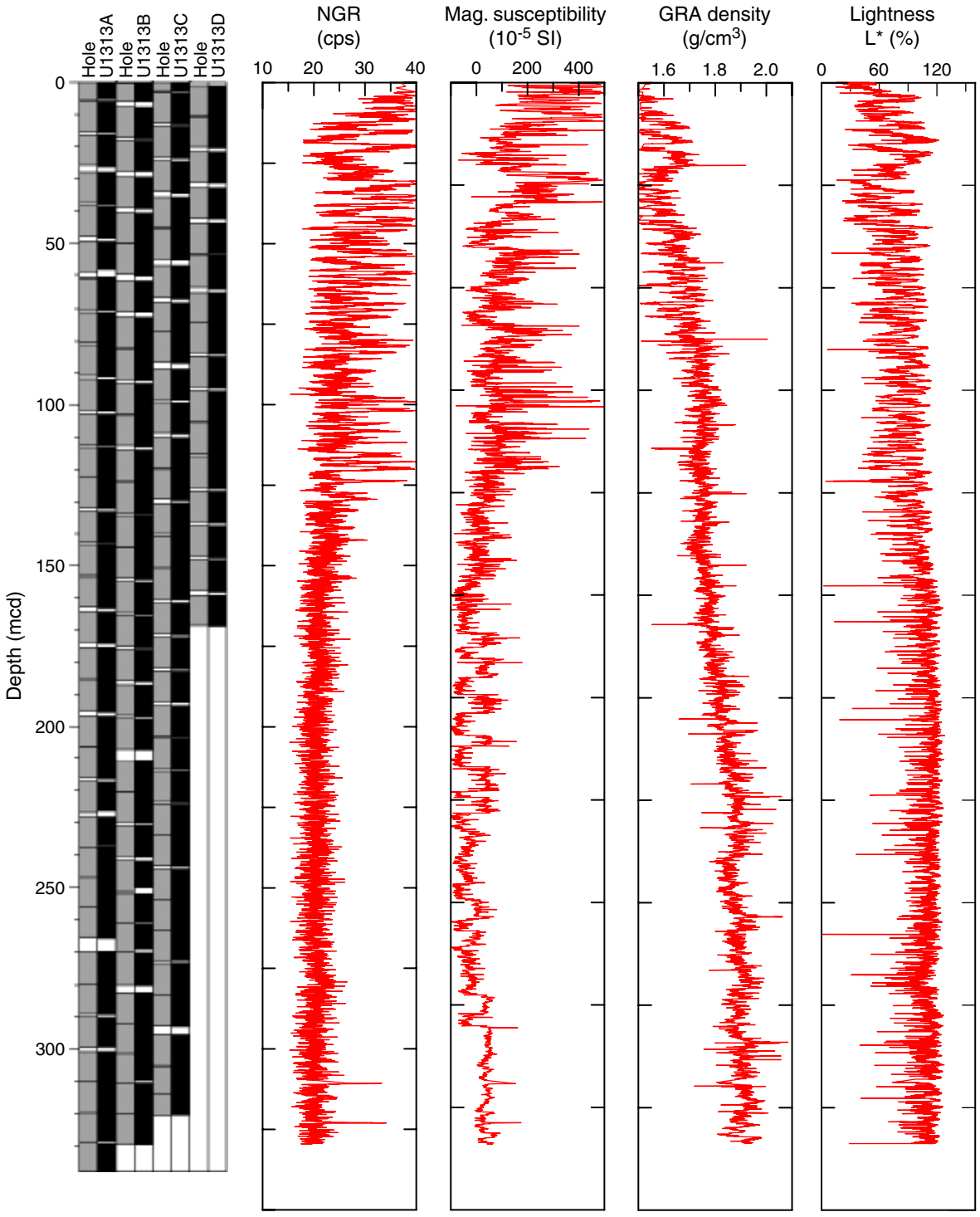

Figure F9. Core recovery, natural gamma ray (NGR) counts, magnetic susceptibility, and gamma ray attenuation (GRA) density measurements from the MST and AMST reflectance (L*) values in the sedimentary record of Site U1314. Gray = cored, black = recovered.